On a self-sustaining process in shear flows

Fabian Waleffe

MIT, Department of Mathematics, Room 2-382, Cambridge, Massachusetts 02139

A self-sustaining process conjectured to be generic for wall-bounded shear flows is investigated. The self-sustaining process consists of streamwise rolls that redistribute the mean shear to create streaks that wiggle to maintain the rolls. The process is analyzed and shown to be remarkably insensitive to whether there is no-slip or free-slip at the walls. A low-order model of the process is derived from the Navier–Stokes equations for a sinusoidal shear flow. The model has two unstable steady solutions above a critical Reynolds number, in addition to the stable laminar flow. For some parameter values, there is a second critical Reynolds number at which a homoclinic bifurcation gives rise to a stable periodic solution. This suggests a direct link between unstable steady solutions and almost periodic solutions that have been computed in plane Couette flow. It is argued that this self-sustaining process is responsible for the bifurcation of shear flows at low Reynolds numbers and perhaps also for controlling the near-wall region of turbulent shear flows at higher Reynolds numbers. © *1997 American Institute of Physics.* [S1070-6631(97)03204-2]

I. INTRODUCTION

Shear flows are a fundamental class of fluid flows. The canonical examples are plane Couette, plane Poiseuille and pipe Hagen–Poiseuille flows. In such simple cases, the Navier–Stokes equations have a simple steady state solution—the laminar state of the flow—in which the velocity is parallel to the walls and varies only in the wall–normal direction. Experimental studies reveal that there is a critical value of the Reynolds number, R_c, below which the laminar state is observed and above which the flow may be "turbulent." This at once suggests an instability of the laminar state, but linear stability analyses lead to the conclusion that the laminar state is stable for all Reynolds numbers.[1,2]

From a general point of view, a shear flow is a nonlinear dynamical system $d\mathbf{u}/dt = f(\mathbf{u}, R)$, the Navier–Stokes equations for incompressible flow with appropriate forcing and boundary conditions, that depends on a single parameter R, the Reynolds number. That dynamical system has one simple fixed point—the laminar state—linearly stable for all R and some mysterious attractor—the turbulent state—when R is larger than some finite R_c. Virtually all initial conditions are attracted to the turbulent state if $R \gg R_c$, while they are attracted to the laminar state if $R \ll R_c$. In fact, it can be shown that there exists a finite Reynolds number $R_e < R_c$ below which the flow tends to the laminar state as $t \rightarrow \infty$, for all initial conditions.[3,4] The proof uses the fact that the nonlinearity in the Navier–Stokes equations conserves the total energy. Hence, the laminar state is the *global* attractor if $R < R_e$ and a *local* attractor for all R. Observations suggest that the laminar state remains a global attractor up to $R = R_c$ after which a mysterious, or perhaps only "strange," attractor emerges. Some of the main objectives are to predict the critical Reynolds number R_c and the R-dependence of turbulent statistics—the momentum transport $\langle uv \rangle$ in particular, as well as to elucidate the structure of the turbulent attractor and the nature of turbulence.

However, the linear stability of the laminar state and the complexity of the turbulent attractor lead to much difficulty in the study of shear flows as our principal tools are based on linear theory. If a linear instability occurs, then a new branch of solution bifurcates from the laminar state and that new branch can be studied by weakly nonlinear analysis in the manner of Malkus and Veronis[5] or Stuart,[6] or by numerical continuation, but the absence of a linear instability prevents those tools from being powered-up.

The lack of exponentially growing linear eigenmodes has led many researchers to go back to the full initial value problem and consider a variety of "transition scenarios." Those scenarios should not be confused with the "routes to chaos" such as the Ruelle–Takens, Feigenbaum period doubling or Pomeau–Manneville routes to chaos.[7] Transition scenarios focus on the temporal sequence of events leading from particular initial conditions to the turbulent attractor. The scenarios do not describe generic sequences of bifurcations of attractors in parameter space, nor do they describe the characteristics of the turbulent attractor. A leading transition scenario has been the evolution from a finite amplitude least stable linear eigenmode plus small random perturbations.[8,9] One of its interests is that it led to the (re-)discovery of the 3D instability of elliptical vortices.[10,11] A different scenario called "bypass transition" has been argued to predominate in less controlled situations. Bypass transition loosely denotes any scenario that does not start with the least stable linear eigenmode. Several bypass scenarios have been studied through numerical simulations of the Navier–Stokes equations (e.g., Ref. 12).

In a similar vein, several researchers have advanced that the key to understanding transition to turbulence in shear flows is to be found in the transient growth associated with the non-normality of the linearized operator (e.g., Refs. 13–15). The idea and results are not new[16,17] (see Ref. 18 for other references) but the formulation is somewhat more general and elegant than earlier studies. Nonetheless, the nonorthogonality of the eigenmodes does not change the fact that the linear analysis is only valid locally and unable to predict global features such as the size of the basin of attraction of the laminar state or the emergence of new attractors not connected to the laminar state.[19,20] Those important questions must consider the particular nonlinearity of the system of

interest. Simple nonlinear models,[14,21,22] illustrating how linear transient growth and ''nonlinear mixing'' could lead to transition, have been shown[19] to violate basic properties of the Navier–Stokes nonlinearity (see also Secs. III and V).

One approach that directly attacks the full nonlinear problem is to look for new fixed points of the dynamical system. In practice, this is extremely difficult as the basic tool—Newton's method—requires a very good initial guess of the fixed point. The primary technique has been *continuation* methods, where one starts from an ''adjacent'' problem for which a nontrivial fixed point is accessible then hopes to follow it through parameter space to the region of interest. Malkus and Zaff[23] used that strategy numerically and experimentally by starting from pressure-driven Ekman flow. This is the flow between two parallel planes rotating around the normal to the planes. By progressively reducing the rotation rate, they managed to track nontrivial solutions back to Poiseuille flow. However, from their experimental observations they concluded that a concurrent spot-like process, unconnected to their new solutions, occurred as plane Poiseuille flow was approached. Nagata[24] started from Taylor–Couette flow in the narrow gap limit which is plane Couette flow rotating around the spanwise direction (parallel to the walls and perpendicular to the flow direction). By following a series of bifurcations, Nagata succeeded in tracking fixed points to nonrotating plane Couette flow. But those solutions survived at Reynolds numbers three times smaller than the R_c observed experimentally and were later found to be unstable by Clever and Busse.[25] No clues have been offered as to the relevance of those solutions and their relation to experiments, until the work reported in Ref. 19. The fixed point continuation approach is a nice procedure, however it requires much artistry and is by no means guaranteed to succeed. The continuation approach also offers limited insight into the nonlinear mechanics of the new solutions.

A different approach based on a detailed mechanistic understanding of the new nonlinear states has been followed by this author together with Kim and Hamilton.[18,19,26,27] Where most previous endeavors focused on transient mechanisms that occur during the transition to turbulence, the objective of this approach was instead to extract those mechanisms that *maintain* the turbulence. From the synthesis of a large body of experimental observations and theoretical work, it has been possible to identify a fundamental self-sustaining process in shear flows. The identification of that process was guided by the conceptual pictures of the ''bursting process'' and associated *horseshoe vortices* observed in turbulent boundary layers[28] as well as by the ''mean flow-first harmonic theory'' proposed by Benney.[29]

The self-sustaining process consists of three distinct phases. First, weak streamwise rolls $[0,V(y,z),W(y,z)]$ redistribute the streamwise momentum to create large spanwise fluctuations in the streamwise velocity $U(y) \rightarrow U(y,z)$. The spanwise inflections then lead to a wake-like instability in which a three-dimensional disturbance of the form $e^{i\alpha x}\mathbf{v}(y,z)$ develops. The primary nonlinear effect resulting from the development of the instability is to reenergize the original streamwise rolls $\mathbf{v}\mathbf{v}^* \rightarrow V(y,z)$, leading to a three-dimensional self-sustaining nonlinear process (Fig. 1).
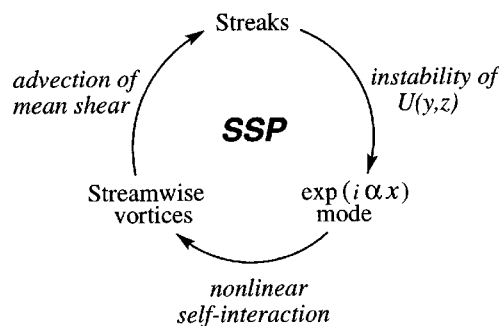

FIG. 1. The self-sustaining process.

This process was first isolated in the form of remarkably organized nearly time-periodic solutions of the Navier–Stokes equations (Figs. 5 and 6 in Ref. 26). Those solutions were obtained by starting from an equilibrated turbulent flow and tracking it down for decreasing box size, a procedure inspired in part by the work of Jimenez and Moin.[30] This tracking procedure amounts to a continuation technique in a three-dimensional parameter space corresponding to the Reynolds number and the periods in the streamwise x and spanwise z directions, but it is a turbulent solution that is tracked instead of fixed points. Further such numerical simulations have been done together with detailed analyses of each phase of the process through a series of controlled numerical simulations of the Navier–Stokes equations (Figs. 2, 3, and 4 in Ref. 27). An eigenmode analysis of the instability of the two-dimensional $U(y,z)$ profile has also been done together with an explicit verification that the nonlinear interaction of the growing eigenmode does indeed feed back on the streamwise rolls.[18] Finally, a low-order model of the process has been proposed[18,19] that may provide a framework to connect the steady solutions in plane Couette flow[24] and the nearly time-periodic solutions.[26,27]

The steady solutions[24] have been tracked down to Reynolds numbers $R \approx 120$ in plane Couette flow but the nearly periodic solutions[26,27] apparently disappear below $R \approx 350$. The latter critical value $R \approx 350$ coincides with that found in experiments[31–33] and computations[34] for larger horizontal domains, in which case the solutions are quite disordered and spot-like. This discrepancy between critical Reynolds numbers led to questions about the relevance, and validity, of the steady solutions. The solutions have been confirmed[25,35] but shown to be unstable. The low-order model has shed some light on this situation as it shows a saddle-node bifurcation, around $R=100$ for some values of the parameters, from which two new steady solutions arise, in addition to the laminar solution, but typically both are unstable. Around $R=350$ however, a global bifurcation of homoclinic type takes place leading to a stable periodic solution.

This paper has two parts. In Sec. II, the self-sustaining cycle (Fig. 1) is cut open and its three phases are studied in succession. That part closely parallels an earlier study.[18] The principal objectives here are to establish the relevant symmetries of the process and to demonstrate its insensitivity to whether there is no-slip or free-slip at the walls. This insensitivity to the boundary conditions underlines the robustness of the process. In the present study we concentrate on steady

Fabian Waleffe

states for each phase as this is more in the spirit of a sustained process than the earlier study that focused on peak streak amplitude and instability growth rate. The symmetries and free-slip boundary conditions are used in the second part of this paper (Sec. III) to derive a low-order model of the self-sustaining process. The low-order model is derived from the Navier–Stokes equations through a truncated Galerkin projection on Stokes modes followed by a physically-motivated reduction. The reduction amounts to projecting the streamwise-dependent part of the flow on the eigenmode of the streak instability instead of Stokes modes. The model is derived for a wall-bounded sinusoidal $\sin \beta y$ shear flow, $|\beta y| \leqslant \pi/2$, with free-slip boundary conditions instead of the more conventional plane Couette and Poiseuille flows with no-slip at the walls. The sinusoidal shear flow with free-slip boundary conditions is better suited to a low-order system modeling as the laminar state is a Galerkin mode and the total energy in the low-order model is then exactly conserved by nonlinear interactions. As will be seen, the self-sustaining process that was first isolated in plane Couette flow also occurs in this sinusoidal shear flow. This is a first explicit verification that the process is generic. The sinusoidal shear flow may actually be a better vehicle for progress in elucidating the nonlinear dynamics of shear flows owing to its greater simplicity.

II. THE THREE PHASES OF THE PROCESS

A. Formation of streaky flow

The simplest element of the self-sustaining process (SSP), Fig. 1, is undoubtedly the streamwise rolls $[0,V(y,z),W(y,z)]$ which decouple from the streamwise velocity $[U(y,z),0,0]$ when the flow is independent of x. In that case the rolls have no energy source and suffer a slow viscous decay. However, the streamwise velocity U is strongly redistributed in y-z planes by the streamwise rolls, as governed by the advection–diffusion equation,

$$\frac{\partial U}{\partial t} + V\frac{\partial U}{\partial y} + W\frac{\partial U}{\partial z} = \frac{1}{R}\nabla^2 U + F(y), \tag{1}$$

where U,V,W do not depend on x and $F(y)$ is a steady deterministic forcing that drives the shear flow if the boundary conditions are homogeneous. The resulting spanwise fluctuations, $U(y,z) - \bar{U}(y)$, are called *streaks*, in reference to the streaks that are observed in experiments when hydrogen bubbles are released along a spanwise wire near the wall in turbulent shear flows.[36] For plane Couette flow, considered in this section, $F=0$ and the flow is driven by the motion of the boundaries $U(y=\pm 1)=\pm 1$ and the laminar state is $U(y)=y$. As usual x, y and z represent Cartesian coordinates in the streamwise, wall–normal and spanwise directions, respectively.

At low Reynolds number, a good guess for the rolls is the lowest-order eigenmode of the operator ∇^4 with boundary conditions $V=\partial V/\partial y=0$ at the walls. This is the operator that appears on the left hand-side of Eq. (6) below. Its even eigenmodes are

$$V(y,z)=V\,\hat{v}(y)\cos\gamma z, \tag{2}$$

where

$$\hat{v}(y)\propto \frac{\cos(py)}{\cos p} - \frac{\cosh(\gamma y)}{\cosh\gamma},$$

normalized so that $\max\hat{v}(y)=1$ and p is a root of $p\tan p + \gamma \tanh \gamma=0$. The spanwise component $W(y,z)$ follows from the continuity equation $\partial V/\partial y + \partial W/\partial z = 0$ and the flow $[0,V(y,z),W(y,z)]$ is an eigenmode of the Stokes operator. The decay rate of those roll eigenmodes is then $(p^2+\gamma^2)/R$, where $p^2+\gamma^2$ has a minimum of 9.27 at $\gamma=1.2$. Such streamwise rolls with the lowest p are shown in Fig. 2 for $\gamma=5/3$. The amplitude of the rolls, V, can then be selected from the criterion that the roll advection rate, V/h, be of the order of the streak diffusion rate $(\beta^2+\gamma^2)\nu/h^2$ with $\beta=\pi/2$, or of its own decay rate $(p^2+\gamma^2)\nu/h^2$, thus selecting the weakest rolls that live long enough to create the strongest (and thus most unstable) streaks. In nondimensional terms, the amplitude of the rolls is $V\approx(\beta^2+\gamma^2)/R$ or $V\approx(p^2+\gamma^2)/R$. For $R=400$, $\gamma=5/3$, these criteria give $V\approx0.013$ and $V\approx0.024$, respectively. With respect to the time dependence of the streamwise rolls, there are two natural choices, either let the rolls decay viscously, or maintain them at their initial amplitude. This second choice was adopted for simplicity and because it is more in the spirit of a sustained process. The mechanism that sustains the streamwise rolls is elucidated in Sec. II C.

From Eq. (1), the effect of the periodic array of streamwise rolls (2) is to induce a spanwise modulation in the streamwise velocity of the form

$$U(y,z)=\sum_{n=0}^{\infty} U_n(y)\cos n\gamma z, \tag{3}$$

such that, with $\hat{v}(y)$ even, $U_{2k}(y)$ has the symmetry of $F(y)$ and $U_{2k+1}(y)$ has the opposite symmetry. For $F(y)$ odd and for Couette flow, $U_n(y)=(-1)^{n+1}U_n(-y)$. In addition to z-reflection $V(y,z)=V(y,-z)$, which implies $U(y,z)=U(y,-z)$ and the cosine expansion in (3), the main symmetry of the rolls is $V(y,z)=-V(-y,z+L_z/2)$, where $L_z=2\pi/\gamma$, from which $U(y,z)=-U(-y,z+L_z/2)$ follows if $F(y)=-F(-y)$.

The $U(y,z)$ profile achieved after about one quarter of the roll's turnover time $t=\pi h/(2V)$, starting from laminar Couette flow at $t=0$, was studied in Ref. 18. That quasi-steady profile is adequate to illustrate the streak instability and the nonlinear feedback on the rolls, but may not be the best choice to model the SSP as it somewhat remembers its initial conditions. Here, the steady state $U(y,z)$ profiles created by steady rolls are considered, in the spirit again that the streamwise rolls and streaks are maintained for all times, on average. Elucidating the mechanism that maintains them is a key objective of this work. Two steady state streaky $U(y,z)$ flow profiles for $V=0.02$ and $V=0.04$ are shown in Fig. 2 for $R=400$. It is interesting to note that for roll amplitudes above the approximate criterion $V=(\beta^2+\gamma^2)/R$, stronger rolls lead to weaker but more localized streaks. The mean profiles $\bar{U}(y)$ corresponding to those streaky flows have an S-shape (Fig. 3) characteristic of turbulent Couette flow with shear rate $d\bar{U}/dy=$ 1.90 at $y=\pm 1$ and 0.03 at
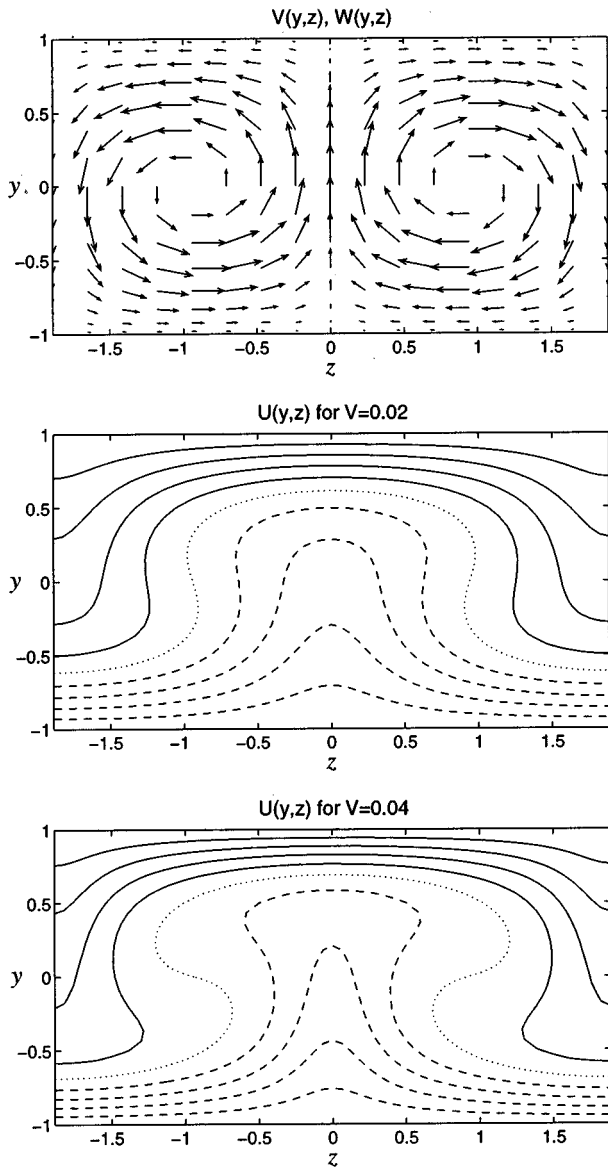
V(y,z), W(y,z)

U(y,z) for V=0.02

U(y,z) for V=0.04

FIG. 2. Redistribution of streamwise velocity U by streamwise rolls $[0,V(y,z),W(y,z)]$ in plane Couette flow at $R=400$ with $\gamma=5/3$. Contours of $U(y,z)$ at 0.2 intervals from -1 at $y=-1$ to 1 at $y=1$. Negative contours dashed, zero contour dotted.

$y=0$ for $V=0.02$, and $d\bar{U}/dy=$ 2.47 at $y=\pm 1$ and -0.16 at $y=0$ for $V=0.04$. Hence, the introduction of streamwise rolls with an amplitude of only 2% of the wall velocity nearly doubled the shear rate at the wall. For roll amplitude larger than about 2% at this $R=400$, the mean velocity profile acquires a negative slope in the center of the channel, and an unstable inflection. It is of course not surprising that streamwise rolls and their associated streaks are so effective at transporting momentum given the results of upper bounds on momentum transport.[37]

B. Instability of streaky flow

The streaky flows $U(y,z)$ (Fig. 2) contain strong spanwise inflections. By analogy with the instability of wakes,[2] one then expects two types of inflectional instability of the
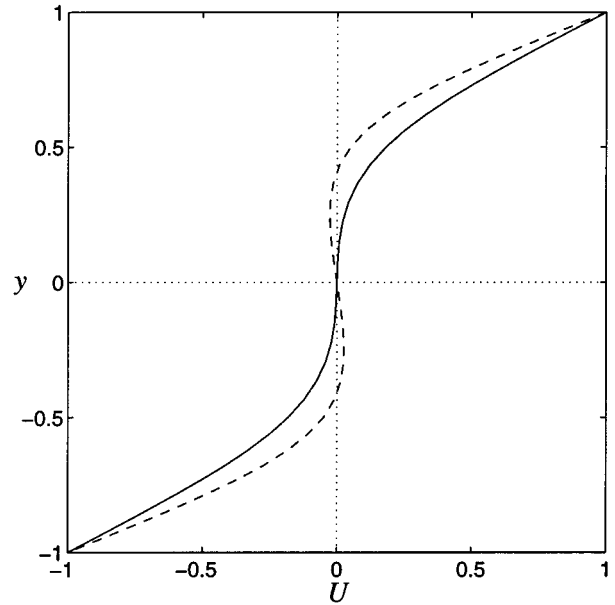

FIG. 3. Mean velocity profiles $\bar{U}(y)$ for $V=0.02$ (solid) and $V=0.04$ (dashed).

streaks, a *fundamental sinusoidal* mode and a *subharmonic "sinucose"* mode[18] as sketched in Fig. 4. There is also a fundamental varicose mode expected to be least unstable. For the near-wall region of turbulent flows the fundamental sinusoidal mode will likely lead to the typical staggered row of vortices as extracted from turbulent data by Stretch,[38] while the subharmonic mode, or the fundamental varicose, would lead to the less frequent *horseshoe* structures.[28,39] Although the symmetric horseshoe structures are more likely to catch the eye, Stretch's data analysis showed that asymmetric structures are typical. This dominance is easily understood in terms of the wake instability analogy that favors the sinusoidal mode.

An eigenmode analysis of the instability of the spanwise varying shear flow $U(y,z)$ was formulated in Ref. 18. Eliminating the pressure from the Navier–Stokes equations linearized around the 2D-1C base flow $U(y,z)\hat{\mathbf{x}}$ by taking the y component of the curl $[\mathbf{j}\cdot\nabla\times(\cdot)]$ and of the curl of the curl $[\mathbf{j}\cdot(\nabla\times(\nabla\times(\cdot)))]$ of the equations yields

$$
\left(\frac{\partial}{\partial t}+U\frac{\partial}{\partial x}-\frac{1}{R}\nabla^2\right)\nabla^2 v+\left(\frac{\partial^2 U}{\partial z^2}-\frac{\partial^2 U}{\partial y^2}\right)\frac{\partial v}{\partial x}+2\frac{\partial U}{\partial z}\frac{\partial^2 v}{\partial x\partial z}
$$
$$
=2\frac{\partial^2}{\partial x\partial y}\left(w\frac{\partial U}{\partial z}\right),
$$
$$
\left(\frac{\partial}{\partial t}+U\frac{\partial}{\partial x}-\frac{1}{R}\nabla^2\right)\eta=\left(\frac{\partial U}{\partial z}\frac{\partial}{\partial y}-\frac{\partial U}{\partial y}\frac{\partial}{\partial z}\right)v \tag{4}
$$
$$
-\left(v\frac{\partial}{\partial y}+w\frac{\partial}{\partial z}\right)\frac{\partial U}{\partial z},
$$

where v and η are the vertical velocity and vorticity, respectively. The u and w velocity components are kinematically determined by v and η from the definition for η, $\partial u/\partial z-\partial w/\partial x=\eta$, and the continuity equation $\partial u/\partial x+\partial w/\partial z=-\partial v/\partial y$.

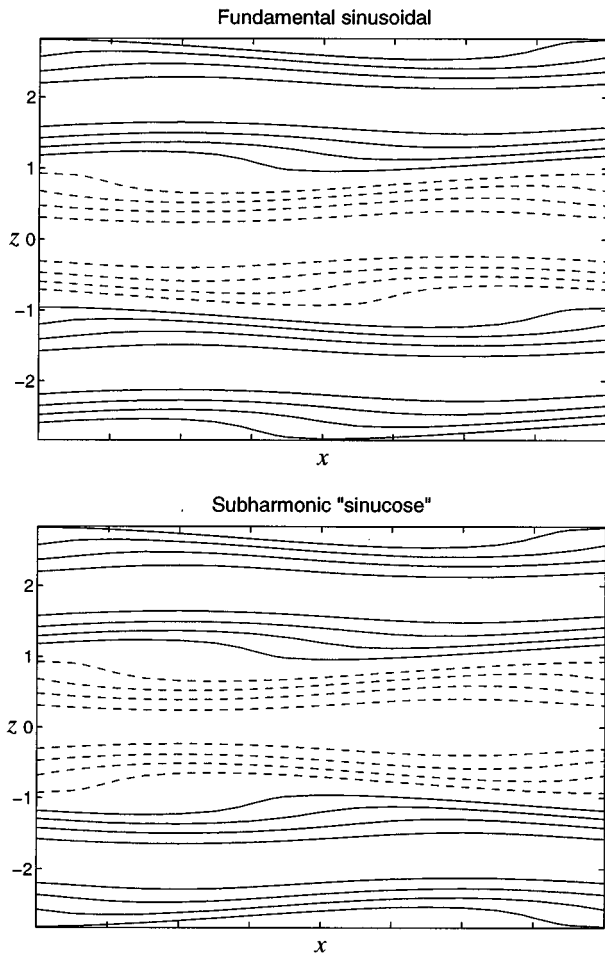Fabian Waleffe

Fundamental sinusoidal

Subharmonic "sinucose"

FIG. 4. Sketch of the two principal modes of instability of the streaky flow $U(y,z)$. Contours of streamwise velocity u (base flow + perturbation) in the $y=0$ plane over 1.5 periods of the base flow in the z-direction.
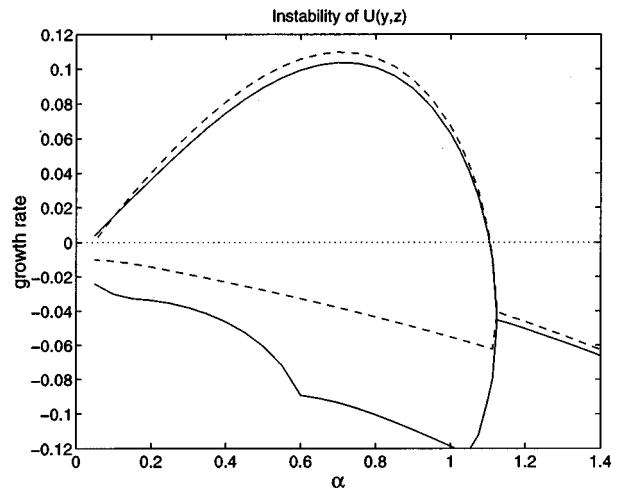

Instability of U(y,z)

FIG. 5. Two largest growth rates for the fundamental sinusoidal instability of the steady state streaky flow $U(y,z)$ corresponding to $V=0.02$, with no-slip (solid) and free-slip (dashed) boundary conditions, vs streamwise wavenumber α, for $\gamma=5/3$, $R=400$.

As mentioned above there are several possible symmetries for the eigensolutions of system (4). Fundamental modes have the same z symmetry as the base flow. Fundamental sinusoidal modes are such that the w component of velocity perturbation is even in z for the even streaks (3); the fundamental varicose mode has a w component that is odd in z for such streaks. Finally, the base flow symmetry $U(y,z)=-U(-y,z+L_z/2)$ implies that if $e^{i\alpha x}[u(y,z),v(y,z),w(y,z)]$ is an eigenmode of Eq. (4) with eigenvalue λ, then $e^{-i\alpha x}[u^*(-y,z+L_z/2), -v^*(-y,z+L_z/2), w^*(-y,z+L_z/2)]$ is an eigenmode with eigenvalue λ^*.

Here as before, the focus is on the fundamental sinusoidal mode of instability of the streaky flow $U(y,z)$, and the velocity perturbations then have the form[18]

$$v = e^{\lambda t} e^{i\alpha x} \sum_{n=1}^{\infty} v_n(y) \sin n\gamma z + \text{c.c.},$$

$$w = e^{\lambda t} e^{i\alpha x} \sum_{n=0}^{\infty} w_n(y) \cos n\gamma z + \text{c.c.},$$

(5)

for the y and z components, where c.c. stands for complex conjugate. The x-component of velocity follows from conti-

nuity. These forms readily include the periodicity and z-symmetry of the fundamental sinusoidal modes. The remaining symmetry implies that if $v_n(y), w_n(y)$ is an eigenmode with temporal eigenvalue λ, then $(-1)^{n+1} v_n^*(-y)$, $(-1)^n w_n^*(-y)$ is an eigenmode with eigenvalue λ^*. In particular, if $\lambda=\lambda^*$ there is an eigenmode with the symmetries $v_n(y)=(-1)^{n+1} v_n^*(-y)$ and $w_n(y)=(-1)^n w_n^*(-y)$, as in Fig. 7.

Results for the fundamental sinusoidal instability of the steady state $U(y,z)$ profile corresponding to $V=0.02$ at $R=400$ are presented here for both no-slip and free-slip boundary conditions at the walls ($u=v=w=0$ or $\partial u/\partial y=v=\partial w/\partial y=0$, at $y=\pm 1$). The spectral computations were done with 33 to 42 Chebyshev polynomials in y and 12 to 14 Fourier wavenumbers in z. The growth rates, $\Re(\lambda)$, for the two most unstable modes are shown in Fig. 5 for both types of boundary conditions. That plot of growth rate versus streamwise wavenumber for the most unstable mode has the shape characteristic of inflectional instabilities of smoothly varying profiles[2] for which there is a high wavenumber cutoff of the order of the typical wavenumber of the base flow (γ in this case). The eigenvalue λ is real for the most unstable mode and thus the mode is nonpropagating.

The lowest-order components $w_0(y)$, $w_1(y)$ and $v_1(y)$ [Eq. (5)] of the most unstable eigenmode for $\alpha=1.1$ are plotted in Fig. 7 and the no-slip and free-slip eigenfunctions are remarkably similar, except of course next to the walls. The reason for choosing $\alpha=1.1$ is that it is approximately the cutoff wavenumber and thus corresponds to a neutral mode for which $\Re(\lambda)=0$. A neutral mode together with the steady rolls and streak constitute an approximate steady equilibrium if it can be shown that the neutral mode feeds back on the rolls. In any case, the shapes of the eigenfunctions are similar for all α below the bifurcation point where the two largest growth rates merge into a complex conjugate pair. Above that point, the overall shapes remain similar but become increasingly asymmetric. The eigenmodes consist
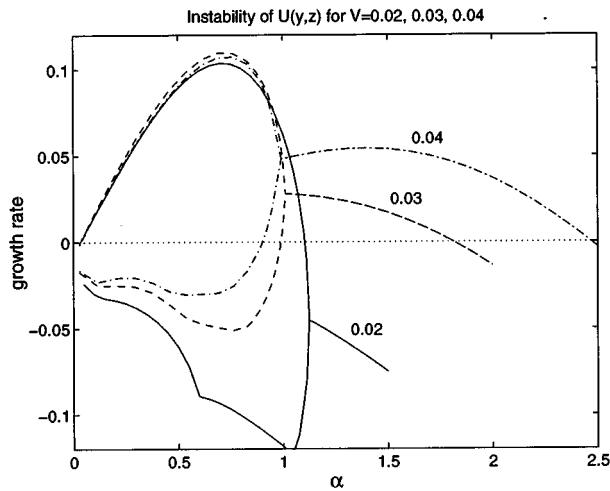
FIG. 6. Two largest growth rates for the fundamental sinusoidal instability of the steady state spanwise-modulated shear flow $U(y,z)$ for no-slip boundary conditions, vs streamwise wavenumber α, for $\gamma=5/3$, $R=400$. Solid: $V=0.02$; dashed: $V=0.03$; dash-dotted: $V=0.04$.

primarily of spanwise velocity (w_0 is largest), as expected for the wake-like instability of the streaks. The structure and growth rate of the most unstable mode are quite insensitive to whether the boundary conditions correspond to free- or no-slip. This similarity between the two types of boundary conditions for the streak instability is very different from the viscous instability described by the Orr–Sommerfeld equation for the plane Poiseuille and Blasius flows which is suppressed by the switch to free-slip at the walls. For the parameters $\alpha=1$, $R=10,000$, the least stable Orr–Sommerfeld mode has growth rate 3.74×10^{-3} with no-slip boundary conditions but -3.52×10^{-2} with free-slip.

The growth rate of the two most unstable fundamental sinusoidal modes of instability of the steady state $U(y,z)$ (Fig. 2) corresponding to $V=0.02$, 0.03 and 0.04, are shown in Fig. 6 for no-slip boundary conditions. For streamwise wavenumber α less than about 1, the eigenvalue for the most unstable mode is real and positive and essentially identical for all three profiles. However, for larger α's there may be a second branch of unstable modes that corresponds to a pair of complex conjugate eigenvalues and the eigenmodes are thus propagating and asymmetric. This new branch of unstable modes is more pronounced as the amplitude of the steady rolls is larger. These propagating unstable modes are probably related to new propagating solutions that have recently been discovered by Nagata[40] in plane Couette flow. In this as in earlier work, the focus is on the nonpropagating modes.

C. Nonlinear feedback on the rolls

The nonlinear feedback of the streak instability on the streamwise rolls, critical to self-sustenance of the process, was first demonstrated in Refs. 18 and 27. A fuller and more precise discussion is provided hereafter. The equation governing the streamwise rolls $\overline{V}^x(y,z)$ reads as

$$\left(\frac{\partial}{\partial t} - \frac{1}{R}\nabla^2\right)\nabla^2\overline{V}^x(y,z) = \frac{\partial^3}{\partial y\,\partial z^2}(\overline{ww}^x - \overline{vv}^x)$$

$$+\left(\frac{\partial^2}{\partial y^2} - \frac{\partial^2}{\partial z^2}\right)\frac{\partial}{\partial z}(\overline{vw}^x), \quad (6)$$

where the overbar $\overline{(\cdot)}^x$ denotes an average over the x-direction. This equation is derived by averaging the Navier-Stokes equations over x then eliminating the pressure and the spanwise velocity component $\overline{W}^x$ through continuity. Equation (6) can be seen as an equation for the average streamwise vorticity $\overline{\omega_x}^x$ as $\nabla^2\overline{V}^x(y,z) = -\partial\overline{\omega_x}^x/\partial z$, however the boundary conditions, $\overline{V}^x = \partial\overline{V}^x/\partial y = 0$ at $y=\pm 1$, are known for $\overline{V}^x$ only.

Substituting the expressions (5) for the fundamental sinusoidal instability of streaky flow $U(y,z)$ onto the right hand side of Eq. (6) forces a $\overline{V}^x(y,z) = \Sigma_{n=1}^{\infty}V_n(y)\cos n\gamma z$, whose first term is $\cos \gamma z$. Hence the z-symmetry is that of the original rolls (2). Writing D for $\partial/\partial y$, the equation for the $\cos \gamma z$ mode reads as

$$\left(\partial_t - \frac{1}{R}(D^2 - \gamma^2)\right)(D^2 - \gamma^2)V_1$$

$$= -\gamma^2 D\left[2w_0w_1^* + \sum_{n=1}^{\infty}(w_nw_{n+1}^* - v_nv_{n+1}^*)\right] + \gamma(D^2$$

$$+\gamma^2)\left[w_0v_1^* + \frac{1}{2}\sum_{n=1}^{\infty}(w_nv_{n+1}^* - w_{n+1}v_n^*)\right] + c.c., \quad (7)$$

where the $*$ denotes a complex conjugate. The y-symmetry of the nonlinear forcing is also correct for feedback on the original rolls. The symmetries for a nonpropagating unstable streak mode, for which $\lambda = \lambda^*$, are such that $v_n(y) = (-1)^{n+1}v_n^*(-y)$ and $w_n(y) = (-1)^nw_n^*(-y)$, as discussed in Sec. II B. It follows directly that the nonlinear forcing on the right hand side of Eq. (7) is even in y. The forced response thus has the correct y and z symmetries to feedback on the original rolls.

However, the correct symmetries do not guarantee feedback as the forcing could have the wrong sign and actually destroy the rolls instead of reenergizing them. To verify feedback explicitly, the right hand side of Eq. (7) is plotted in Fig. 8 together with $(D^2 - \gamma^2)\hat{v}(y)$, which is $(D^2 - \gamma^2)V_1$ for the original rolls (2). At first sight, the nonlinear forcing (''W''shape) is quite different from the original $(D^2 - \gamma^2)V_1$ (''V'' shape), however upon closer inspection it is clear that there is a good correlation between the two functions. A different display of the same information is given in Fig. 13 of Ref. 27. The feedback can be demonstrated in a different way by comparing the forced response of Eq. (7) to the original profile for the rolls $\hat{v}(y)$ Eq. (2). This is done in Fig. 9 and streamwise rolls almost identical to the original rolls are generated by the nonlinear forcing resulting from the streak eigenmode.

The cycle has been closed. The steady rolls lead to steady streaks that lead to a neutral mode that generates steady rolls. For a neutral streak mode, $\Re(\lambda)=0$ and the
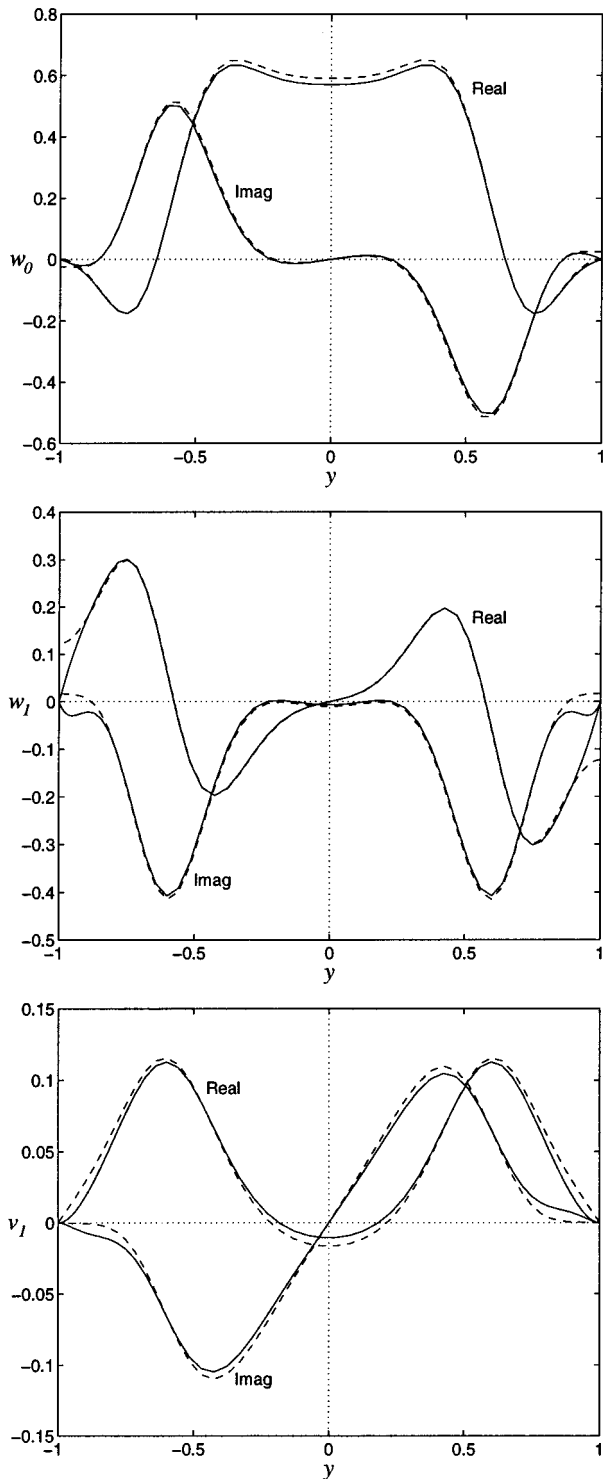
FIG. 7. Principal components w_0, w_1 and v_1 of the unstable eigenmode of the streak instability with $v = e^{i\alpha x}\Sigma_n v_n(y)\sin n\gamma z$, and $w = e^{i\alpha x}\Sigma_n w_n(y)\cos n\gamma z$ [Eq. (5)], for $\alpha = 1.1$, $\gamma = 5/3$, $R = 400$. Solid: no-slip, dashed: free-slip.

right hand side of Eq. (7) is steady. Here the neutral mode is also a steady mode, $\mathfrak{R}(\lambda) = \mathfrak{I}(\lambda) = 0$. By focusing on steady rolls and streaks and a neutral mode, an approximate steady equilibrium has been determined. The amplitude of the neutral mode is the last remaining unknown and it could be determined such that the amplitude of the steady forced re-

sponse to Eq. (7) equals the original amplitude of the rolls, $V = 0.02$.

It is worth noting that the wavenumber $\alpha = 1.1$ for the neutral mode corresponds well to the wavenumber $\alpha = 1.14$ that was determined by the turbulent solution tracking procedure.[27] The spanwise wavenumber $\gamma = 5/3$ was chosen to correspond to those numerical solutions. The streak stability results, Fig. 5, and the numerical solutions suggest that when the minimum α allowed in the domain is less than the cutoff wavenumber for the streak instability, then the Navier–Stokes solution is disordered. If the minimum allowed wavenumber is larger than the cutoff, then the "turbulent" solution is not sustained and the flow returns to laminar.

The three phases of the SSP, formation of streaks by streamwise rolls, streak instability and feedback on the rolls, are described by the three equations (1), (4) and (6), respectively. However, those equations are not complete to describe the interactions between the three phases. Equation (1) lacks the Reynolds stress terms $\partial\overline{uv}^x/\partial y + \partial\overline{vw}^x/\partial z$ that extract energy from $U(y,z)$ to sustain the growth of the streak instability. Equations (4) lack the interaction between the rolls $V(y,z)$ and the streak disturbance (u,v,w) that extract energy from the latter to sustain the rolls. To put it differently, Eqs. (1) and (4) describe the actions without the reactions. A complete model of the SSP is derived in the next section.

III. LOW-ORDER MODEL OF THE PROCESS

A. Lowest-order Galerkin projection

A complete but low-order model of the self-sustaining process is derived here for a sinusoidal shear flow driven in the x direction by $F(y) = F\sin\beta y$, $\beta = \pi/2$, with free-slip boundary conditions at $y = \pm 1$. This sinusoidal shear flow is best suited to low-order Galerkin projections as the appropriate expansion functions are Fourier modes in all three coordinates. Another advantage is that the mean flow is a low-order mode and the total energy is then exactly conserved by Galerkin truncation at any order. Free-slip boundary conditions are also routinely considered in Rayleigh–Bénard convection. Lengths are nondimensionalized by the half-channel height h and velocities by the laminar root-mean-square (rms) velocity. The nondimensional amplitude of the force is then $F = \sqrt{2}\beta^2/R$. The reader may worry that the resulting laminar flow, $U(y) = \sqrt{2}\sin\beta y$, is inflectional (Fig. 10), but that inflection does not lead to instability because of the wall blocking. Indeed, Tollmien considered such a flow to show that Rayleigh's inflection point theorem is necessary but not sufficient for inviscid instability.[2] The wall-bounded sinusoidal shear flow with free-slip at the walls is then a simple parallel shear flow for which the laminar state is stable for all Reynolds numbers, as in plane Couette and pipe Poiseuille flows.

The streamwise rolls can be chosen in the simple form $V(y,z) \propto \cos\beta y \cos\gamma z$, with $W(y,z)$ by continuity. The symmetries of the spanwise varying mean flow $U(y,z)$ are as discussed in the previous section, Eq. (3). The lowest-order truncation for the x-independent flow then consists of
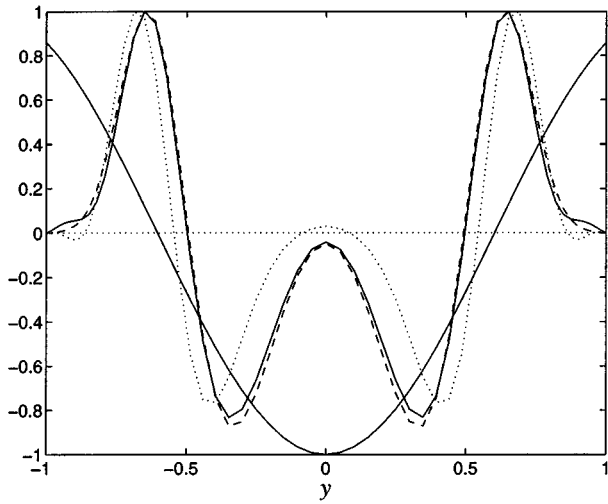
FIG. 8. Feedback on streamwise rolls: solid ''V'' shape is $(D^2 - \gamma^2)\hat{v}(y)$, ''W'' shapes are the nonlinear forcing on the RHS of Eq. (7) owing to the fundamental sinusoidal unstable streak mode, for $\alpha = 1.1$, $\gamma = 5/3$, $R = 400$. Solid: no-slip eigenmode; dashed: free-slip eigenmode. The dotted W-shape is the contribution from no-slip w_0, w_1 and v_1 only.

$$\begin{pmatrix} U(y,z) \\ V(y,z) \\ W(y,z) \end{pmatrix} = M\Psi_{010} + U\Psi_{001} + V\Phi_{011}, \qquad (8)$$

with

$$\Psi_{010} \propto \begin{pmatrix} \sin \beta y \\ 0 \\ 0 \end{pmatrix}, \quad \Psi_{001} \propto \begin{pmatrix} \cos \gamma z \\ 0 \\ 0 \end{pmatrix},$$

$$\Phi_{011} \propto \begin{pmatrix} 0 \\ \gamma \cos \beta y \cos \gamma z \\ \beta \sin \beta y \sin \gamma z \end{pmatrix},$$

where the amplitudes of the mean shear M, the streaks U and the rolls V, are real functions of time. The modes Ψ_{lmn}, Φ_{lmn} are normalized to have a unit mean square, such that
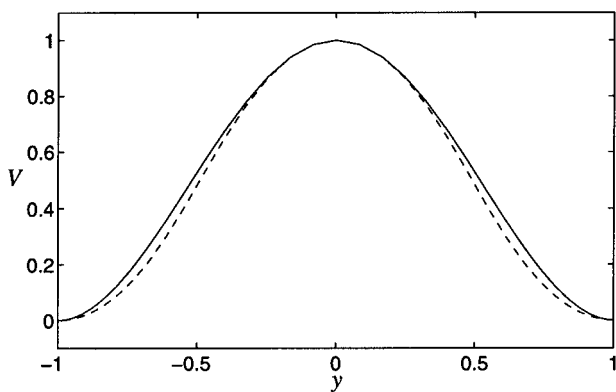

FIG. 9. Comparison of the streamwise rolls created from the nonlinear forcing, Eq. (7), by the neutral fundamental sinusoidal streak eigenmode and the original rolls, Eq. (2), for $\alpha = 1.1$, $\gamma = 5/3$, $R = 400$. Original rolls: solid, forced response: dashed.
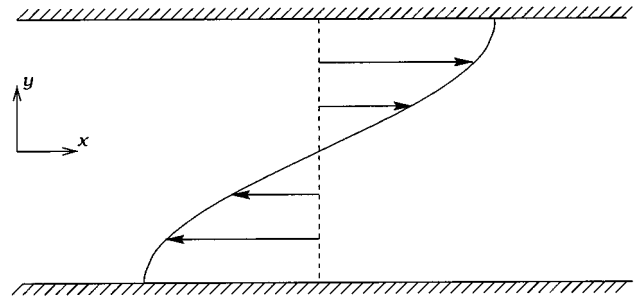
FIG. 10. Sketch of the $\sin \beta y$ wall-bounded shear flow considered for the Galerkin projection with free-slip boundary conditions.

the mean square velocity is the sum of the squares of the amplitudes. The Ψ_{lmn} modes are streak, or vertical (i.e., y) vorticity, modes with no vertical velocity and wavenumbers $l\alpha$, $m\beta$ and $n\gamma$ in the x, y and z directions, respectively. The Φ_{lmn} modes are roll, or vertical velocity, modes with no vertical vorticity. Both sets of modes are divergence-free.

The lowest-order truncation for the streak instability mode, incorporating the symmetries of the fundamental sinusoidal mode [Eq. (5)], consists of keeping only those modes associated with w_0, w_1 and v_1 in (5) (see also Fig. 8). This truncation for the x-dependent part of the flow then consists of

$$e^{i\alpha x}\mathbf{v}(y,z) + \text{c.c.} = A\Psi_{100} + B\Psi_{101} + C\Psi_{110} + D\Psi_{111}$$
$$+ E\Phi_{111}, \qquad (9)$$

where

$$\Psi_{100} \propto \begin{pmatrix} 0 \\ 0 \\ \cos \alpha x \end{pmatrix}, \quad \Psi_{110} \propto \begin{pmatrix} 0 \\ 0 \\ \sin \alpha x \sin \beta y \end{pmatrix},$$

are the modes associated with w_0,

$$\Psi_{101} \propto \begin{pmatrix} -\gamma \cos \alpha x \sin \gamma z \\ 0 \\ \alpha \sin \alpha x \cos \gamma z \end{pmatrix},$$

$$\Psi_{111} \propto \begin{pmatrix} \gamma \sin \alpha x \sin \beta y \sin \gamma z \\ 0 \\ \alpha \cos \alpha x \sin \beta y \cos \gamma z \end{pmatrix},$$

are the modes associated with w_1, and

$$\Phi_{111} \propto \begin{pmatrix} \alpha\beta \sin \alpha x \sin \beta y \sin \gamma z \\ (\alpha^2 + \gamma^2)\cos \alpha x \cos \beta y \sin \gamma z \\ -\beta\gamma \cos \alpha x \sin \beta y \cos \gamma z \end{pmatrix},$$

corresponds to v_1. The amplitudes A, B, C, D, E are real functions of time with the modes normalized as previously.

The lowest-order consistent truncation of the velocity field that may capture the self-sustaining process consists of the eight modes defined in (8) and (9) and keeps three wavenumbers $(-1, 0$ and $1)$ in all three directions. Although this is undoubtedly a severe truncation, much of the reduction

comes from the symmetries identified in the previous section. Without those symmetries the same level of truncation would yield 52 modes $[2*(3^3-1)]$.

The governing equations are derived by substituting the expansion (8) plus (9) for $\mathbf{u}$ in the Navier–Stokes equations:

$$\left(\frac{\partial}{\partial t}-\frac{1}{R}\nabla^2\right)\mathbf{u}=-\mathbf{u}\cdot\nabla\mathbf{u}-\nabla p+F(y)\hat{\mathbf{x}},$$

and projecting onto each mode (Galerkin projection). The modes of the expansion satisfy the continuity equation $\nabla\cdot\mathbf{u}=0$ and the boundary conditions $\partial u/\partial y=v=\partial w/\partial y=0$ at $y=\pm 1$ with $\mathbf{u}=(u,v,w)$; hence the pressure p drops out of the final equations. In general if

$$\mathbf{u}=\sum_{l,m,n}[A_{lmn}(t)\Phi_{lmn}(\mathbf{x})+B_{lmn}(t)\Psi_{lmn}(\mathbf{x})],$$

where the expansion functions Φ_{lmn},Ψ_{lmn} are orthogonal eigenmodes of the Stokes operator, $\nabla^2\{\Phi,\Psi\}_{lmn}=-\kappa_{lmn}^2\{\Phi,\Psi\}_{lmn}$ with $\nabla\cdot\{\Phi,\Psi\}_{lmn}=0$, the equation for A_{lmn} is

$$\left(\frac{d}{dt}+\frac{\kappa_{lmn}^2}{R}\right)A_{lmn}=-\langle(\mathbf{u}\cdot\nabla\mathbf{u})\cdot\Phi_{lmn}\rangle+\langle F(y)\hat{\mathbf{x}}\cdot\Phi_{lmn}\rangle,$$

where the brackets $\langle\ \rangle$ denote a spatial average, and the wavenumber $\kappa_{lmn}^2=l^2\alpha^2+m^2\beta^2+n^2\gamma^2$. There is a similar equation for B_{lmn} with Ψ in place of Φ. For the eight modes defined in (8), (9), the Galerkin projection yields

$$\left(\frac{d}{dt}+\frac{\kappa_m^2}{R}\right)M=\frac{-\beta\gamma}{\kappa_d}BE+\frac{\beta\gamma}{\kappa_v}UV+\frac{\kappa_m^2}{R},$$

$$\left(\frac{d}{dt}+\frac{\kappa_u^2}{R}\right)U=\frac{\gamma^2}{\kappa_b}AB-\frac{\gamma^2}{\kappa_b}CD-\frac{\alpha\beta\gamma}{\kappa_b\kappa_d}CE-\frac{\beta\gamma}{\kappa_v}MV,$$

$$\left(\frac{d}{dt}+\frac{\kappa_v^2}{R}\right)V=\frac{2\alpha\beta\gamma}{\kappa_b\kappa_v}(AD+BC)+\frac{\alpha^2\beta^2-\gamma^2\kappa_d^2}{\kappa_b\kappa_d\kappa_v}AE,$$

$$\left(\frac{d}{dt}+\frac{\kappa_a^2}{R}\right)A=-\alpha CM-\frac{\alpha^2}{\kappa_b}BU-\frac{\alpha\beta\gamma}{\kappa_b\kappa_v}DV$$
$$-\frac{\alpha^2\beta^2}{\kappa_b\kappa_d\kappa_v}EV,$$

$$\left(\frac{d}{dt}+\frac{\kappa_b^2}{R}\right)B=\alpha DM+\frac{\beta\gamma}{\kappa_d}EM+\frac{\alpha^2-\gamma^2}{\kappa_b}AU$$
$$-\frac{2\alpha\beta\gamma}{\kappa_b\kappa_v}CV,$$

$$\left(\frac{d}{dt}+\frac{\kappa_c^2}{R}\right)C=\alpha AM+\frac{\alpha^2}{\kappa_b}DU-\frac{\alpha\beta\gamma}{\kappa_b\kappa_d}EU,$$

$$\left(\frac{d}{dt}+\frac{\kappa_d^2}{R}\right)D=-\alpha BM+\frac{\gamma^2-\alpha^2}{\kappa_b}CU-\frac{\alpha\beta\gamma}{\kappa_b\kappa_v}AV,$$

$$\left(\frac{d}{dt}+\frac{\kappa_e^2}{R}\right)E=\frac{2\alpha\beta\gamma}{\kappa_b\kappa_d}CU+\frac{\gamma^2\kappa_d}{\kappa_b\kappa_v}AV,$$

$$(10)$$

with the wavenumbers

$$\beta=\pi/2,$$

$$\kappa_m^2=\beta^2,\quad \kappa_u^2=\gamma^2,\quad \kappa_v^2=\beta^2+\gamma^2,$$

$$\kappa_a^2=\alpha^2,\quad \kappa_b^2=\alpha^2+\gamma^2,\quad \kappa_c^2=\alpha^2+\beta^2,\quad \kappa_d^2=\alpha^2+\beta^2+\gamma^2,$$

$$\kappa_e^2=\kappa_d^2.$$

B. Analysis of the truncated system

The eighth-order truncation (10) embodies many of the characteristics of shear flows. From a global point of view, the nonlinearity is quadratic and energy conserving. The evolution of the total energy results only from the forcing and viscous dissipation. Writing A_i, $i=1,\ldots,8$ for the amplitudes $M,\ldots,E$ in (10) the total energy obeys

$$\frac{d}{dt}\sum_{i=1}^{8}A_i^2=\frac{\kappa_1^2}{R}A_1-\frac{1}{R}\sum_{i=1}^{8}\kappa_i^2A_i^2.$$

A statistically steady state is possible only if $0<A_1\equiv M\leq 1$, otherwise the total energy decays. No unbounded growth is possible as the quadratic dissipation of energy always dominates the linear energy input for sufficiently large amplitude. These global properties hold for any level of truncation.

Locally, the dynamics is such that the mean shear M and the rolls V are linearly stable, but the streaks U have two modes of instability. Linearizing the system around a state where all modes are zero except the mean M, amounts to setting $U=V=0$ in the equations for the x-dependent modes A,B,C,D,E and setting the latter modes to zero in the equations for the x-independent flow M,U,V. It is quickly verified from the skew-symmetry of the ACM and BDM interactions that there are no exponentially growing modes on the mean M. The inviscid linear stability of the mean shear is a general result of Tollmien as recalled at the beginning of the previous section. There are two transient algebraically growing modes arising from the MV term in the U equation and from the EM term in the B equation, but neither one triggers nonlinear effects that lead to bifurcation of the flow. Both are indeed incomplete representations of a passive advection-diffusion process such as described by Eq. (1) with decoupling between the streaks and the rolls. The MV term is the redistribution of the mean shear M by the rolls V leading to transient algebraic growth of U. This is balanced by the UV term in the M equation and there is no nonlinear feedback on the streamwise rolls V. Likewise the EM term in the B equation is balanced by the BE term in the M equation and there is no nonlinear feedback on the pair of oblique rolls E, as discussed in Ref. 18. The complete B,D,E,M interaction corresponding to the transient growth of B for instance is governed by

Phys. Fluids, Vol. 9, No. 4, April 1997

Fabian Waleffe   891

$$\left(\frac{d}{dt}+\frac{\kappa_m^2}{R}\right)M=\frac{\kappa_m^2}{R}-\frac{\beta\gamma}{\kappa_d}BE,$$

$$\left(\frac{d}{dt}+\frac{\kappa_b^2}{R}\right)B=\alpha DM+\frac{\beta\gamma}{\kappa_d}EM,$$

$$\left(\frac{d}{dt}+\frac{\kappa_d^2}{R}\right)D=-\alpha BM,\qquad\qquad(11)$$

$$\left(\frac{d}{dt}+\frac{\kappa_e^2}{R}\right)E=0,$$

whose only attractor is the laminar point $M=1$, $B=D=E=0$. The interaction between M,U,V is similar [cf. Eq. (14) in Ref. 18], reflecting the exact decoupling of the roll V that is not sustained [Eq. (1)].

Linearizing around some finite streamwise roll V with all other modes infinitesimal (assuming for instance that the roll V is forced instead of the mean M), yields the same conclusion that there are no exponentially growing modes on the roll V. Here again, there are transient algebraically growing modes that do not trigger nonlinear effects leading to bifurcation. One transient arises from the CV term in the B equation, balanced by the BV term in the V equation with no feedback on C. Two other transients arise from the interaction of the modes A, D, E through the roll V. The decoupling that prevents nonlinear feedback is less obvious but still present in this case. It is most easily seen by rewriting the interaction between those 4 modes in terms of interaction between the modes A, V and $\widetilde{D}\equiv D+\alpha\beta E/(\gamma\kappa_d)$ and $\widetilde{E}\equiv E-\alpha\beta D/(\gamma\kappa_d)$, in which case the interaction reads as

$$\left(\frac{d}{dt}+\frac{\kappa_v^2}{R}\right)V=\frac{\alpha\beta\gamma}{\kappa_b\kappa_v}A\widetilde{D}-\frac{\gamma^2\kappa_d}{\kappa_b\kappa_v}A\widetilde{E}+\frac{\kappa_v^2}{R},$$

$$\left(\frac{d}{dt}+\frac{\kappa_a^2}{R}\right)A=-\frac{\alpha\beta\gamma}{\kappa_b\kappa_v}\widetilde{D}V,$$

$$\left(\frac{d}{dt}+\frac{\kappa_d^2}{R}\right)\widetilde{D}=0,\qquad\qquad(12)$$

$$\left(\frac{d}{dt}+\frac{\kappa_e^2}{R}\right)\widetilde{E}=\frac{\alpha^2\beta^2+\gamma^2\kappa_d^2}{\kappa_b\kappa_d\kappa_v}AV.$$

One transient mode corresponds to the growth of A from the $\widetilde{D}V$ term in the A equation with no feedback on $\widetilde{D}$. The other transient mode results from the growth of $\widetilde{E}$ with $\widetilde{D}=0$ through the AV term in the $\widetilde{E}$ equation with no feedback on A. The only attractor for this subsystem is $V=1$, $A=D=E=0$ and, again, the transients do not lead to bifurcation. This lack of direct nonlinear ''recycling of outputs into inputs,'' illustrated by the 5 explicit examples above, is generic[41] and has been one of the arguments against the simple picture of transition,[14,22] and even turbulence[15] as ''linear transient growth with nonlinear mixing.''

In contrast to the linear stability of M and V, the linear analysis of finite amplitude streaks U reveals two modes of instability. From (10), the equations for the x-dependent modes A,B,C,D,E when $M=V=0$ with U a finite constant,

decouple into two sets corresponding to the interaction through the streaks U of modes A,B, even in y, and of modes C,D,E, odd in y.

The linearized equations for the even modes A,B are

$$\left(\frac{d}{dt}+\frac{\kappa_a^2}{R}\right)A=\frac{-\alpha^2}{\kappa_b}BU,$$

$$\left(\frac{d}{dt}+\frac{\kappa_b^2}{R}\right)B=\frac{\alpha^2-\gamma^2}{\kappa_b}AU,\qquad(13)$$

which reduce to the second-order equation,

$$\left(\frac{d}{dt}+\frac{\kappa_b^2}{R}\right)\left(\frac{d}{dt}+\frac{\kappa_a^2}{R}\right)A=\alpha^2\frac{\gamma^2-\alpha^2}{\gamma^2+\alpha^2}U^2A\qquad(14)$$

[cf., Ref. 18 Eq. (20)] and there is exponential instability whenever $\gamma>\alpha$ provided R is large enough. In the inviscid limit, $R\to\infty$, the unstable eigenmode is $B/A=-\delta_1\ \mathrm{sign}(U)/\alpha$ with growth rate $\alpha\delta_1|U|/\kappa_b$ where $\delta_1^2=\gamma^2-\alpha^2$. Likewise, the linearized equations for the odd modes C,D,E reduce to the second-order equation,

$$\left(\frac{d}{dt}+\frac{\kappa_d^2}{R}\right)\left(\frac{d}{dt}+\frac{\kappa_c^2}{R}\right)C=\alpha^2\frac{\gamma^2-\alpha^2-\beta^2}{\gamma^2+\alpha^2+\beta^2}U^2C,\qquad(15)$$

and there is instability if $\gamma^2>\alpha^2+\beta^2$ and R is large enough. Equation (15) is equivalent to Eq. (14) with $\alpha^2\to\alpha^2+\beta^2$. This is a direct consequence of Squires' theorem.[2]

In summary, the mean shear M and the rolls V are both linearly stable while the streaks U have two modes of instability, one even and one odd in y. This implies that the primary mechanism to exchange energy between the x-independent modes M,U,V and the x-dependent modes A,B,C,D,E is through the streak instabilities. In agreement with the general description of the self-sustaining process, one sees that the forcing of the shear M can be transferred to the streaks U by the rolls V through the MV term in the U equation. The x-dependent modes can then develop from the instability of the streaks U. Inspection of the V equation shows that the feedback on the rolls V arises from the nonlinear interaction between the even (A,B) and odd (C,D,E) modes of instability of the streaks. This points to an important secondary role of the mean M which is to break the y-symmetry in order to couple the two modes of instability of the streaks in such a way that feedback on the streamwise rolls occurs.

C. Reduction of the truncated system

The truncated eighth-order system (10) can be further reduced by imposing relationships between the even modes A, B and between the odd modes C, D and E that correspond to the most unstable eigenstructures for the streak instabilities, Eqs. (14), (15). The streak instability is inviscid in nature and the eigenstructures are taken in the inviscid limit, $R\to\infty$. This imposes three kinematic constraints relating B to A and C and D to E,

$$B=\mathscr{C}_{ba}A,\quad C=\mathscr{C}_{ce}E,\quad D=\mathscr{C}_{de}E,\qquad(16)$$

where

Fabian Waleffe

$$\mathscr{C}_{ba} = \frac{-\delta_1}{\alpha} \text{sign}(U), \quad \mathscr{C}_{ce} = \frac{\kappa_b \delta_2}{2\beta\gamma} \text{sign}(U),$$

$$\mathscr{C}_{de} = \frac{\kappa_d \delta_1^2}{2\alpha\beta\gamma}, \tag{17}$$

with $\delta_1^2 = \gamma^2 - \alpha^2$ and $\delta_2^2 = \gamma^2 - \alpha^2 - \beta^2$. The eigenstructures are chosen hereafter to correspond to the instability of positive streaks $U>0$. By symmetry there is an equivalent system for negative streaks.

To preserve the symmetry of the equations, the amplitudes and the decay rates are rescaled such that $A \rightarrow (1+\mathscr{C}_{ba}^2)^{-1/2}A$, $E \rightarrow (1+\mathscr{C}_{ce}^2 + \mathscr{C}_{de}^2)^{-1/2}E$, $(\kappa_a^2 + \mathscr{C}_{ba}^2\kappa_b^2)/(1+\mathscr{C}_{ba}^2) \rightarrow \kappa_a^2$, $(\kappa_e^2 + \mathscr{C}_{ce}^2\kappa_c^2 + \mathscr{C}_{de}^2\kappa_d^2)/(1+\mathscr{C}_{ce}^2 + \mathscr{C}_{de}^2) \rightarrow \kappa_e^2$. The sign of V is also changed at this point $V \rightarrow -V$ for the purpose of presentation. The truncated eighth-order model (10) then reduces to the fifth-order model,

$$\left(\frac{d}{dt} + \frac{\kappa_m^2}{R}\right)M = \sigma_{mae}AE - \frac{\beta\gamma}{\kappa_v}UV + \frac{\kappa_m^2}{R},$$

$$\left(\frac{d}{dt} + \frac{\kappa_u^2}{R}\right)U = \frac{-\alpha\delta_1}{\kappa_b}A^2 - \frac{\alpha\delta_2}{\kappa_d}E^2 + \frac{\beta\gamma}{\kappa_v}MV,$$

$$\left(\frac{d}{dt} + \frac{\kappa_v^2}{R}\right)V = \sigma_{vae}AE, \tag{18}$$

$$\left(\frac{d}{dt} + \frac{\kappa_a^2}{R}\right)A = \frac{\alpha\delta_1}{\kappa_b}AU - \sigma_{aem}EM + \sigma_{aev}EV,$$

$$\left(\frac{d}{dt} + \frac{\kappa_e^2}{R}\right)E = \frac{\alpha\delta_2}{\kappa_d}EU + \sigma_{eam}AM - \sigma_{eav}AV,$$

where all coefficients σ are positive definite, except σ_{aev}, and $-\sigma_{aem} + \sigma_{eam} + \sigma_{mae} = \sigma_{aev} - \sigma_{eav} + \sigma_{vae} = 0$, thus preserving conservation of energy by the nonlinear term. The mean M is linearly stable. To preserve linear stability of V it is necessary that $\sigma_{aev} \geq 0$.

The meaning of this reduction is clear. The x-dependent part of the flow field is now represented in terms of (an approximation to) the unstable streak modes instead of the eigenmodes of the Stokes operator. One limitation of this new expansion is that as written it is only valid for $\delta_2^2 = \gamma^2 - \alpha^2 - \beta^2 \geq 0$, which seems too restrictive from a physical point of view. It amounts to requiring instability of both the even and odd (in y) streak modes, but the growth of the even mode A from the streak instability (i.e., through the $\alpha\delta_1/\kappa_b AU$ term with $\delta_1^2 = \gamma^2 - \alpha^2 > 0$) should suffice to drive the system with the odd mode E arising from the interaction of the even mode with the mean shear through the $\sigma_{eam}AM$ term. That interaction is in fact required to insure that A and E will be positively correlated in order to feedback on the rolls V, as discussed hereafter. Another simple reduction that corresponds to choosing a neutral inviscid odd mode is

$$\mathscr{C}_{ba} = \frac{-\delta_1}{\alpha}\text{sign}(U), \quad \mathscr{C}_{ce} = 0, \quad \mathscr{C}_{de} = \frac{\beta\gamma}{\alpha\kappa_d}. \tag{19}$$

The reduced system (18) indicates quite clearly that the feedback on the rolls results from the interaction between the even (A) and odd (E) streak modes. The reduction was chosen to correspond to the instability of $U>0$ thus V must be positive to sustain $U>0$ by redistribution of the mean shear $M>0$. It follows that A and E must have the same sign to sustain $V>0$. A further reduction can then be made by choosing for instance $W/\sqrt{2} = A = E$ and $\kappa_w^2 = (\kappa_a^2 + \kappa_e^2)/2$, in which case the equations reduce to the fourth-order system,

$$\left(\frac{d}{dt} + \frac{\kappa_m^2}{R}\right)M = \sigma_m W^2 - \sigma_u UV + \frac{\kappa_m^2}{R},$$

$$\left(\frac{d}{dt} + \frac{\kappa_u^2}{R}\right)U = -\sigma_w W^2 + \sigma_u MV,$$

$$\left(\frac{d}{dt} + \frac{\kappa_v^2}{R}\right)V = \sigma_v W^2, \tag{20}$$

$$\left(\frac{d}{dt} + \frac{\kappa_w^2}{R}\right)W = \sigma_w UW - \sigma_m MW - \sigma_v VW,$$

where all coefficients σ are positive. One of those coefficients (σ_u for instance), could be normalized to unity by changing the time scale but this will not be done in the following. Analytic expressions for the coefficients are given in the Appendix for both reductions. Reduction (17) requires $\delta_1^2 = \gamma^2 - \alpha^2 > 0$, $\delta_2^2 = \gamma^2 - \beta^2 - \alpha^2 > 0$, while reduction (19) requires $\delta_1^2 = \gamma^2 - \alpha^2 > 0$ and $\gamma^2 - \beta^2 > 0$ otherwise instability of the streaks and/or feedback on the rolls are not possible.

Model (20) preserves the global properties of the earlier systems. The nonlinear term conserves energy; there is no unbounded growth and a statistically steady state is possible only for $0 < M \leq 1$. The mean M is still linearly stable while negative rolls $V<0$ are unstable to W and positive rolls $V>0$ are stable. The only term that can extract energy from the mean is the UV term provided $UV>0$ but only $V>0$ can be sustained by the $\sigma_v W^2$ term. In that case energy can be transferred from the mean M to the streaks U through the MV term. The streak instability then gives rise to W through the $\sigma_w UW$ term and the nonlinear self-interaction of W sustains the rolls V through the $\sigma_v W^2$ term. Note that the mean shear M reduces the streak instability through the $-\sigma_m MW$ term and that there is an associated nonlinear feedback, $\sigma_m W^2$, on M. With regards to the three phases of the SSP, the formation of streaks [Eq. (1)] is represented by the M and U equations with $W=0$, the instability of the streaky flow [Eq. (4)] is represented by the W equation with $V=0$ and the feedback on the rolls [Eq. (6)] is represented by the V equation.

Model (20) is identical to the model proposed in Refs. 18 and 19, except for the extra interaction between the mean M and the streak mode W. That interaction had been omitted in the original model.

D. Analysis of the fourth-order model

The characteristics of model (20) are quite similar to those of the original model[18,19] which is identical to (20) with $\sigma_m = 0$. In addition to the laminar point $M=1$,

$U=V=W=0$ there are two other fixed points if R is larger than some critical value R_{sn}. Eliminating M, V and U from equations (20) with $d/dt=0$, the fixed points are determined by the roots of the cubic,

$$\sigma_u^2\sigma_v^4 X^3 + \kappa_w^2\sigma_u^2\sigma_v^2 X^2 + (\kappa_u^2\kappa_v^2\sigma_m^2 + \kappa_m^2\kappa_v^2\sigma_w^2 + \kappa_m^2\kappa_u^2\sigma_v^2)X$$
$$+ \kappa_m^2 R(\kappa_u^2\sigma_m - \sigma_u\sigma_v\sigma_w X) + \kappa_m^2\kappa_u^2\kappa_w^2 = 0, \qquad (21)$$

where $X=(RW/\kappa_v)^2$. This equation is most easily used to determine R as a function of $X\geq 0$, $R(X)$, which is the ratio of a positive definite cubic in X and a linear term in X. There is a $R>0$ for all X such that

$$\sigma_u\sigma_v\sigma_w X > \kappa_u^2\sigma_m. \qquad (22)$$

The function $R(X)$ has a unique minimum over all X satisfying (22). That minimum is the critical Reynolds number R_{sn} at which a *saddle-node* bifurcation takes place. For $R>R_{sn}$ there are two real solutions $X>0$ to the cubic (21).

The main effect of the nonzero σ_m is to bound the lower branch of new solutions away from the laminar solution $M=1$, $U=V=W=0$ as the asymptotic scaling of the lower branch as $R\to\infty$ is

$$M\to\frac{1}{1+(\kappa_u^2/\kappa_m^2)\ (\sigma_m^2/\sigma_w^2)}, \quad U\to\frac{\sigma_m}{\sigma_w}M,$$
$$V=O(R^{-1}), \quad W=O(R^{-1}), \qquad (23)$$

instead of

$$M\to 1, \quad U=O(R^{-1}), \quad V=O(R^{-2}),$$
$$W=O(R^{-3/2}), \qquad (24)$$

when $\sigma_m=0$. The presence of $\sigma_m>0$ is thus quite significant for the conjecture that an amplitude $\epsilon=O(R^{-a})$ with a strictly larger than 1 is sufficient to cause transition.[14,22] The scaling of the upper branch is as reported earlier,[19] $M=O(R^{-1})$, $U=O(R^{-1/2})$, $V=O(R^{-1/2})$ and $W=O(R^{-3/4})$ as $R\to\infty$.

The stability analysis of the fixed points involves finding the eigenvalues for the linearization of model (20) around those fixed points. The eigenvalues are the roots of the fourth-order characteristic polynomial. All coefficients of that polynomial are positive except for the linear term that is indefinite and the constant term that is equal to $2R^2W^2\partial\mathscr{C}/\partial X$ where $\mathscr{C}(X)$ is the cubic defined in (21). If that constant term is negative then there is one real positive root and the fixed point is unstable. The lower branch of solutions which corresponds to the smallest of the two positive roots of the cubic (21) is thus a saddle-point as $\partial\mathscr{C}/\partial X<0$ for that root. The upper branch may be unstable if the coefficient of the linear term of the characteristic polynomial is sufficiently negative for that larger root. In such cases there are two positive real eigenvalues and that root is an unstable node.

The smallest Reynolds number at which the saddle-node bifurcation takes place is $R_{sn}=104.84$ at $\alpha=1.30$, $\gamma=2.28$, for the reduction (17), and $R_{sn}=137.17$ at $\alpha=1.49$, $\gamma=1.82$ for the reduction (19) (Fig. 11). The two largest real parts of the eigenvalues governing the stability of the upper branch of solutions are shown in Fig. 12 for both reductions

as functions of R. For R just above critical there are two real positive eigenvalues that quickly merge into a pair of complex eigenvalues with positive real part indicating a switch from an unstable node to an unstable spiral. The other two eigenvalues (not shown) are complex conjugates with a larger negative real part. In both cases the upper branch is an unstable node near the bifurcation. That unstable node turns into an unstable spiral after only a slight increase of R, to 104.94 and 137.33, respectively, beyond R_{sn} (see the blow-up in Fig. 12). The positive real part of the eigenvalues decreases as R increases and the spiral fixed point becomes stable at $R_{Hf}=138.06$ and 180.24, for both reductions, respectively. This implies a Hopf bifurcation at those Reynolds number where the spiral fixed point collides with a limit cycle.

The collision between the spiral fixed point and the limit cycle may occur in two ways. Either the unstable spiral point bifurcates into an unstable limit cycle surrounding the stable spiral, or the unstable spiral is surrounded by a stable limit cycle and collides with it leading to a stable spiral. In the latter case, the stable limit cycle has to be generated at a lower value of R and it could arise from a *homoclinic bifurcation*. The first scenario in which an unstable limit cycle is generated is the scenario that takes place for the parameter values corresponding to Fig. 12. The second scenario, involving a homoclinic bifurcation, can also occur in model (20) for different values of the parameters.

That second, more dramatic, dynamical behavior is illustrated in Fig. 13. For R below R_{sn}, the laminar state (solid black dot) is the only fixed point. That fixed point is linearly stable with nonorthogonal eigenvectors and remains such for all R. At $R=R_{sn}$, a saddle-node bifurcation introduces two new fixed points, a saddle and an unstable node [open circles, Fig. 13(a)], but almost all initial conditions still end up at the laminar fixed point. For R slightly greater than R_{sn}, the unstable node turns into an unstable spiral [Fig. 13(b)]. As R increases, the spiral tightens and a homoclinic bifurcation takes place at $R=R_{hc}$ [Fig. 13(c)]. This gives rise to a stable limit cycle which is a significant attractor for the flow in phase space [Fig. 13(d)]. Many initial conditions now settle onto the periodic orbit instead of the laminar fixed point. A global bifurcation has taken place.

The coefficients corresponding to reduction (17) and to the minimum R_{sn} for $\alpha=1.30$, $\gamma=2.28$, are $[\sigma_m,\sigma_u,\sigma_v,\sigma_w]=[0.31,1.29,0.22,0.68]$, with the decay rates $[\lambda_m,\lambda_u,\lambda_v,\lambda_w]=[2.47,5.20,7.67,7.13]$. The coefficients chosen in Refs. 18 and 19 are $[\sigma_m,\sigma_u,\sigma_v,\sigma_w]=[0,1,1,0.5]$, with the decay rates $[\lambda_m,\lambda_u,\lambda_v,\lambda_w]=[10,10,10,15]$. For those values a more complex behavior is observed near R_{sn}. The upper branch is stable from $R_{sn}=98.63$ to $R=100.02$ where it loses stability in a Hopf bifurcation. The ensuing stable limit cycle disappears in a homoclinic bifurcation at $R=101.03$ beyond which the only stable attractor is the laminar fixed point up until a second homoclinic bifurcation that takes place near $R\approx 356$ and reintroduces a stable limit cycle. From a practical point of view those extra stable attractors between $R_{sn}=98.63$ and $R=101.03$ are insignificant because of their minute basins of attraction, but in any case it is interesting to note that they
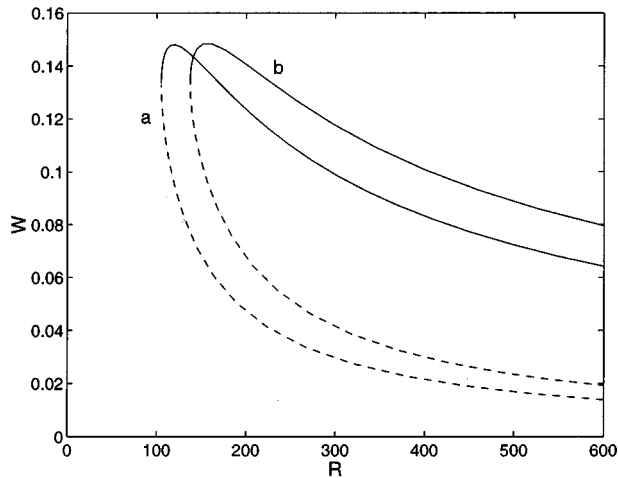
FIG. 11. Bifurcation diagram showing the amplitude of W vs R for the two nontrivial steady solutions of the fourth-order model (20) for (a) reduction (17) and (b) reduction (19). Upper branch solid, but not necessarily stable; lower branch saddle-point dashed.

FIG. 13. Phase plane illustration of some possible dynamics for model (20). The solid black dot is the stable laminar solution. The two open circles are the two steady solutions, Eq. (21). (a) R just above R_{sn}: saddle and unstable node; (b) $R_{hc} > R > R_{sn} + \epsilon$: saddle and unstable spiral; (c) $R = R_{hc}$: homoclinic bifurcation; (d) $R > R_{hc}$: stable limit cycle.

are removed for σ_m larger than about 0.025, all other parameters being unchanged, see Fig. 14. The occurrence of the homoclinic bifurcation appears to depend strongly on the value of σ_m. The reader is referred to Refs. 18 and 19 for plots of the homoclinic bifurcation and the stable limit cycle that appears near $R = 356$, for those parameter values.

IV. DISCUSSION

In summary, there is a critical Reynolds number R_{sn} for the fourth-order model (20) where a saddle-node bifurcation introduces two new steady solutions (Fig. 11) in addition to the laminar solution. Those solutions are typically *both* unstable, with the lower branch corresponding to a saddle point with a single positive real eigenvalue, and the upper branch
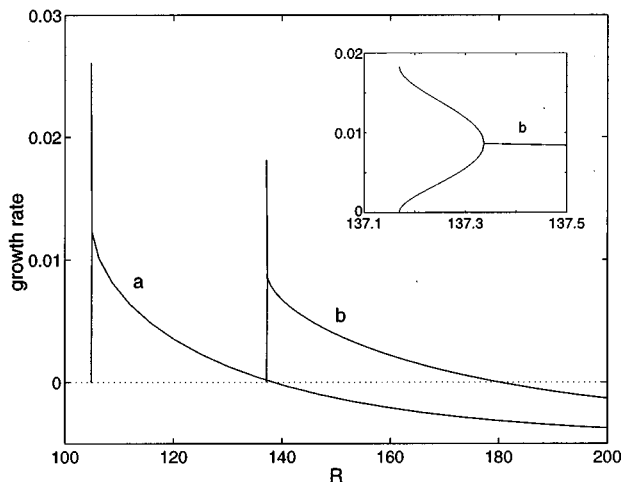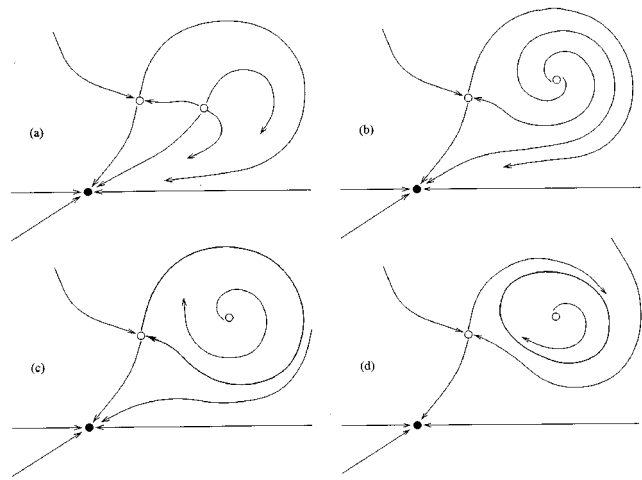

FIG. 12. Two largest growth rates for the instability of the upper branch of nontrivial steady solutions of the fourth-order model (20) for (a) reduction (17) with $\alpha = 1.30$, $\gamma = 2.28$ and (b) reduction (19) with $\alpha = 1.49$, $\gamma = 1.82$. The insert is a blow-up of (b) near R_{sn}.

corresponding to an unstable node with two real positive eigenvalues. As R is increased, the unstable node quickly turns into an unstable spiral (Figs. 12 and 14). These features of the model are particularly interesting in light of the discovery of unstable steady solutions in plane Couette flow.[24,25] The spiral node may become stable through a Hopf bifurcation at some $R = R_{Hf}$ (Fig. 12). For different values of the parameters, a homoclinic bifurcation may introduce a stable periodic solution (Fig. 13). This latter scenario is particularly interesting in light of the discovery of nearly periodic solutions in plane Couette flow.[26,27]

These connections between the behaviors observed in the low-order model (20) and the results for the Navier–Stokes equations in the case of plane Couette flow hence provide some evidence for the validity and applicability of the low-order model. Nonetheless, a main issue is to determine whether the low-order model features are artifacts of the severe truncation or indeed valid representations of the Navier–Stokes dynamics for shear flows. A first step is to look for those features in the original eighth-order model (10). An extensive study of the eighth-order model has not been done but it would appear that there are no other fixed points nor attractors in that model besides the laminar point. Closer inspection shows that the mean flow M *enhances* the instability of the streaks U in the eighth-order model and correlates the even (A-B) and odd (C-D-E) modes of instability incorrectly for feedback on the rolls V to occur. In the fourth-order model the mean shear M reduces the streak instability, in fact, exponential growth of W is possible only if $\sigma_w U > \sigma_m M$. A reduction of the streak instability by the mean shear has also been shown[42] for the full streak instability problem (4). The cause of the anomalous enhancement of the streak instability by the mean shear, and the subsequent lack of a self-sustaining process, in the eighth-order model appears to be the incorrect representation, at that order of truncation, of the shearing effect of the mean $M \sin \beta y \hat{\mathbf{x}}$ on the x-dependent modes A, B, C, D.

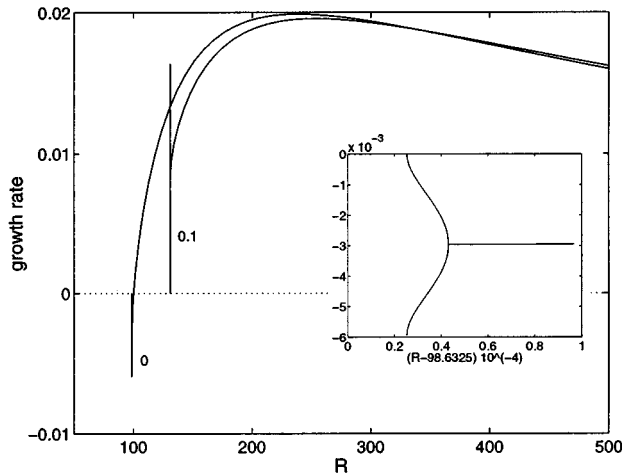Phys. Fluids, Vol. 9, No. 4, April 1997

Fabian Waleffe   895

FIG. 14. Two largest growth rates for the instability of the upper branch of nontrivial steady solutions of the fourth-order model (20) for $\sigma_m = 0$ and $\sigma_m = 0.1$ with $[\sigma_u, \sigma_v, \sigma_w] = [1,1,0.5]$, $[\lambda_m, \lambda_u, \lambda_v, \lambda_w] = [10,10,10,15]$ in both cases. The insert is a blow-up of the $\sigma_m = 0$ case near R_{sn}.

To illustrate that anomalous behavior, consider the simple case of the advection of a passive scalar ϕ by the mean shear as governed by

$$\frac{\partial \phi}{\partial t} + M \sin \beta y \frac{\partial \phi}{\partial x} = 0. \qquad (25)$$

The exact solution of that equation for initial conditions $\phi(\mathbf{x}, 0) = \cos \alpha x$ is simply $\phi(\mathbf{x}, t) = \cos \alpha(x - Mt \sin \beta y)$. Near $\beta y = n\pi$, the wavenumber in the y direction increases like $\alpha \beta M t$ and there is a "cascade" towards higher wavenumbers owing to the differential advection by the shear flow. The y-wavenumber remains close to zero near $\beta y = (2n+1)\pi/2$ where there is no shear. For short times, $\phi(\mathbf{x}, t) \sim \cos \alpha x + \alpha M t \sin \alpha x \sin \beta y + O(t^2)$, these two terms correspond to the modes A and C in Eq. (9). Projecting Eq. (25) onto those two modes with $\phi(\mathbf{x}, t) = A \cos \alpha x + C \sin \alpha x \sin \beta y$ yields

$$\dot{A} = -\alpha C M/2,$$
$$\dot{C} = \alpha A M, \qquad (26)$$

which is identical to the corresponding interaction in Eq. (10) after the renormalizations $A \rightarrow \sqrt{2}A$, $C \rightarrow 2C$, $M \rightarrow \sqrt{2}M$. Although the single triad interaction ACM, Eq. (26), preserves the global property of Eq. (25) that the average of ϕ^2 is conserved, its dynamics, which consists of rotation at rate $\alpha M/\sqrt{2}$, is not a correct representation of the actual dynamics of a cascade in wavenumber space at the shear rate βM. This misrepresentation of differential advection by a single triad has been discussed before (cf., Ref. 43, Sec. VII) and two triads are needed to adequately represent the differential advection which corresponds to advection in wavenumber space.

This discussion of the lowest-order truncation of equation (25) indicates that the interactions between the mean and the x-dependent modes that arise from advection by the

mean shear—the ACM and BDM interactions—in the eighth-order model (10) are inadequate. However, the full Navier–Stokes dynamics for the SSP does not correspond either to a wavenumber increase in the y-direction. The SSP is a fully nonlinear state—not just a linear passive-scalar advection by the mean as in Eq. (25) — such that this shearing does not occur for two reasons. First, the streamwise rolls and streaks, being x-independent, are not sheared by the mean. In fact, it is the mean that is passively advected by the rolls, Eq. (1), and is largely wiped out by the streamwise rolls and streaks (Fig. 3). Second, the x-dependent modes involved in the SSP form an eigenstructure that arises from the instability of the streaky flow $U(y, z)$, which consists of the mean shear and the streaks (Sec. II B). By definition, the eigenstructure is not sheared by the mean, just as eigenmodes of the Rayleigh and Orr–Sommerfeld equations are not sheared by the mean.

Except for the advection by the mean, the other interactions are adequately represented by the eighth-order truncation in (10). The redistribution of streamwise momentum by the streamwise rolls, Eq. (1), is well represented by the MUV interaction. That interaction is indeed the rotation at rate $\propto \gamma V$ of the shear in the y direction into shear in the z direction [cf., Ref. 18, Fig. 2 and Eq. (11)]. The streak instability and the feedback on the rolls also appear to be adequately represented by low-order truncations [cf., Ref. 18 Eqs. (19) and (20)]. This is because those phases are essentially "modal" as discussed above and in Secs. II B and II C. The ACM and BDM interactions that inadequately represent the interactions with the mean in the eighth-order model (10) cancel completely or substantially in the reductions (17) or (19), respectively, that lead to the fourth-order model (20). This probably explains why the fourth-order model may better represent the actual Navier–Stokes dynamics than the truncated eighth-order model.

The main consequence of the anomalous behavior in the eighth-order model is that it is not possible to directly reduce the eighth-order model (10) to the fourth-order model (20). If the instability of the streaky flow $U(y, z)$, consisting of both M and U, was well-behaved in the eighth-order model then it would be possible to link all the x-dependent modes A–E into a single streaky flow eigenmode as in Secs. II B and II C. Instead, it was necessary to first reduce the eighth-order model to a fifth-order model by combining A, B and C, D, E as dictated by the even and odd eigenmodes of the streaks U only, that is $U(y, z) - \bar{U}(y)$. The fifth-order model was then reduced to a fourth-order model by imposing an arbitrary relation between the two streak modes, $A = E$, in (18). In general, this introduces an undetermined parameter $\mathscr{C}_{ae} > 0$ where $A = \mathscr{C}_{ae} E$.

This discussion naturally suggests that the number of modes should be increased in the y-direction at least, to avoid this misrepresentation by the Galerkin truncation of the interaction with the mean. The next level of truncation keeps four modes in the y direction and leads to a 17th-order system which is too large to handle analytically but numerical investigations reveal a saddle-node bifurcation near $R = 100$ with both solutions unstable, as in the fourth-order model and plane Couette flow. The unstable steady solutions

Fabian Waleffe

persist as the resolution is increased further and have been continued up to a Galerkin truncation involving 92 modes so far, after reduction arising from symmetries. Those solutions, continued to even higher resolutions, will be reported upon in a forthcoming paper. It is not yet known whether the homoclinic bifurcation that leads to a stable periodic solution persists for those higher-order truncations. A better way to derive the fourth-order model (20), avoiding the anomalous behavior of the eighth-order model, would thus be to use for (9) the projection of the eigenstructure obtained from a higher-order truncation onto the five modes defined in (9).

V. COMPARISON WITH OTHER MODELS

There is a small overlap between this self-sustaining process and linear transient growth[14] at the level of the simplest phase of the process: the formation of streaks by streamwise rolls (Sec. II A). The work on linear transient growth approximates Eq. (1) and emphasizes the transient algebraic growth of the streaks, but the complete physics is the passive advection–diffusion of streamwise velocity by the rolls which is adequately described by the transients only for $\epsilon R \ll 1$, where ϵ is a measure of the amplitude of the rolls (Ref. 18, Sec. 3). The work on transient growth has not addressed, nor identified, the other two more complex phases of the process: the streak instability and the feedback on the streamwise rolls. Discussion of the crucial nonlinear feedback necessary for transition has been limited to *ad hoc* low-order models,[14,21,22] except for the earlier work of Benney and Gustavsson.[16,26] The proposed low-order models call on some artificial nonlinear couplings not present in the Navier–Stokes equations and ignore (or crudely model[21]) the important feedback on the mean[19] (see also Sec. III B). At the level of the low-order model (20), this amounts to setting $M=1$, $W=0$, ignoring the M equation and adding a $-V\sqrt{U^2+V^2}$ term to the U equation and a $U\sqrt{U^2+V^2}$ term to the V equation to "recycle outputs into inputs."[14] This transforms the fourth-order model (20) into

$$\left(\frac{d}{dt}+\frac{\kappa_u^2}{R}\right)U = \sigma_u V - V\sqrt{U^2+V^2},$$
$$\left(\frac{d}{dt}+\frac{\kappa_v^2}{R}\right)V = U\sqrt{U^2+V^2}.$$
(27)

A complete nonlinear analysis of model (27), with a more realistic nonlinearity that has U in place of $\sqrt{U^2+V^2}$, has been made by Dauchot and Manneville.[20]

Another class of low-order models of shear flow dynamics are those based on the *Proper Orthogonal Decomposition* (POD).[44–47] The POD models are derived from the Navier–Stokes equations by a Galerkin projection, as for the model derived in this paper. However, the POD modes impose artificial kinematic constraints between the two degrees of freedom for the velocity field—the "roll" and "streak" modes of Sec. III A. This is best understood at the level of the first phase of the process: the formation of streaks by streamwise rolls (Sec. II A). The streaky flow $[U(y,z),0,0]$ and the streamwise rolls $[0,V(y,z),W(y,z)]$ are kinematically independent. Dynamically, the streaky flow $U(y,z)$ is controlled by the rolls, Eq. (1), but the latter remain independent of the streaky flow. In the POD models, the streaks and the rolls are linked into a single mode. This results in an artificial direct feedback on the rolls and a spurious linear instability of the laminar flow. The POD models have also typically ignored the dynamics of the mean, although they include the Reynolds stress which then leads to a triple nonlinearity that stops the artificial exponential growth. In the fourth-order model (20), this amounts to setting $dM/dt=W=0$ and $V=\tau U$. The fourth-order model then reduces to the single equation,

$$(1+\tau^2)\frac{d}{dt}U + \frac{\kappa_u^2+\tau^2\kappa_v^2}{R}U = \sigma_u\tau U\left(1-\frac{R\sigma_u\tau U^2}{\kappa_m^2}\right),$$
(28)

with the spurious exponential growth term ($\sigma_u\tau U$ term) and the cubic nonlinearity that prevents unbounded growth. The artificial kinematic constraints appear in all POD models, including those that involve x-dependent modes.[45,47] The kinematic constraints could be removed as explained in Ref. 19, Sec. V.

Recall that W in model (20) is the amplitude of the x-dependent streak instability mode. The other variables M, U, V represent the mean shear, the streamwise streaks and the streamwise rolls, respectively. When $W=0$, the laminar state is the global attractor for model (20) because the rolls are not sustained, as in the full Navier–Stokes dynamics when the flow is independent of x. Models (27) and (28) sustain the rolls through artificial couplings between the streaks and the rolls. Model (27) uses a nonlinear dynamical coupling while model (28) uses a linear kinematic coupling.

VI. CONCLUSIONS

A self-sustaining process (SSP) in shear flows where streamwise rolls redistribute the mean shear to create streaks that break down to recreate the rolls, has been studied and shown to be remarkably insensitive to whether there is free-slip or no-slip at the walls. A complete model of the process has been derived by projecting the Navier–Stokes equations on an appropriate set of orthogonal modes. The derived model is essentially similar to one previously proposed.[18,19]

The model provides a template for understanding and elucidating the Navier–Stokes dynamics of shear flows. Unstable steady solutions[24,25] that exist down to $R \approx 120$ and nearly time-periodic solutions[26,27] that apparently exist down to $R \approx 350$ have recently been found in plane Couette flow. Similarly in the low-order model, a saddle-node bifurcation at $R=R_{sn}$ introduces two fixed points that are typically both unstable. For some values of the parameters, a homoclinic bifurcation takes place at $R=R_{hc}>R_{sn}$ that introduces a stable periodic solution (Fig. 13). The quantitative agreement between the critical values of the Reynolds numbers in the fourth-order model and the full Navier–Stokes case may even be excellent, $R_{sn} \approx 100$, and $R_{hc} \approx 350$ has been observed in the fourth-order model.[19] However, anomalous behavior in the eighth-order Galerkin truncation (10) prevents

Phys. Fluids, Vol. 9, No. 4, April 1997

Fabian Waleffe   897

direct reduction to the fourth-order model (20) and forces the introduction of an arbitrary parameter (Sec. IV).

The homoclinic bifurcation scenario provides a plausible simple link between the unstable steady solutions in plane Couette flow[24,25] and the nearly periodic solutions.[26,27] This work thus suggests a reinvestigation of the solutions computed in Refs. 27 and 28 to determine whether truly time-periodic solutions do exist in plane Couette flow and whether they arise from a homoclinic bifurcation. The period of the cycle should diverge like $|\ln(R-R_{hc})|$ as the homoclinic bifurcation is approached from above.[48] The global nature of a homoclinic bifurcation also adds to the possible relevance of this scenario to the bifurcation of shear flows. Experiments on transition to turbulence in shear flows seem to indicate that a broad range of initial conditions tend to the turbulent state when $R>R_c$ while all initial conditions seem to return to the laminar state when $R<R_c$. Hence, experiments seem to indicate a global bifurcation, although elucidating that point has not been the focus of most studies. Recent experiments along these lines have been made by Dauchot and Daviaud.[49]

To isolate the SSP in the numerical simulations, we restricted the class of solutions to those that are periodic in x and z over short periods, $L_x \approx 6h$ and $L_z \approx 4h$. This cannot be done experimentally but other ingenious set-ups may lead to an experimental verification of the SSP. Dauchot, Bottin and Daviaud[49,50] have studied plane Couette flow modified by a spanwise wire in the limit of the wire thickness tending to zero. They observe the formation of streaks by streamwise rolls followed by the oscillation and break-up of the streaks in an intermittent cycle. This is reminiscent of behavior observed in early numerical simulations[51] when the x and z periods were not quite tuned properly. Further adjustments of the spatial periods led closer to time-periodic solutions.[26,27]

In those recent experiments,[49,50] the streamwise vortices are generated by the spanwise wire. One important aspect of this and earlier work[18,27] is to elucidate the nonlinear mechanism for the generation of streamwise vortices. The generation of streamwise streaks from streamwise vortices is a simple mechanism that has long been understood, but the origin of the vortices themselves remained a mystery. It has been shown that the streamwise vortices directly result from the nonlinear development of an instability of the streaks. The latter instability is driven by the inflections of the streaky flow $U(y,z)$ in the z-direction. The new information that emerges from the derivation of the low-order model is that the feedback on the streamwise rolls results from the nonlinear interaction between an even and an odd, in y, mode of instability of the streaks. An important secondary role of the mean shear is to break the y symmetry and correlate those two modes in such a way that feedback on the rolls is realized. This explains why streamwise rolls do not spontaneously arise in classical inflectional instabilities of a pure $U(z)$ profile, as in the Kelvin–Helmholtz roll-up of unbounded shear layers.

On this issue of the mechanism for the generation of streamwise vortices, it is worth emphasizing that it is an instability of the streaks, not of the rolls, that drives the process. This is illustrated by the analysis of the truncated model (Sec. III B). In the Taylor–Couette problem, a linear instability introduces the streamwise Taylor vortices. A secondary instability then leads to wavy vortices. As a result, one often reads about instability of streamwise vortices in the plane shear flow context. But an instability of the rolls would provide another energy drain in addition to viscosity. The crucial element in shear flows was actually to discover the mechanism that *sustains* the rolls against viscous decay.

Finally, with respect to the issue of turbulent disorder, an interesting feature of this work and the associated Navier–Stokes calculations[27] is that it has been possible to isolate an organized process that is responsible for strongly increased momentum transport (Fig. 3). Thus the turbulent disorder and the increased shear at the wall have been dissociated. The momentum transport is not due to a molecular-like disordered process but results instead from an organized process. In fact, it is possible that the disorder actually reduces the momentum transport allowed by the Navier–Stokes dynamics as realized by the self-sustaining process. This reduction of the transport is also suggested by the upper bound results.[37] As for the disorder, it may arise through the Ruelle–Takens–Newhouse scenario.[7] If the picture of a homoclinic bifurcation (Fig. 13) leading to a limit cycle indeed applies to the Navier–Stokes equations, the limit cycle could bifurcate into quasiperiodic motion (2-torus) and from there to a strange attractor.

The self-sustaining process is expected to retain some relevance to the dynamics of shear flows throughout those further bifurcations as the Reynolds number and/or the x and z periods are increased. The process was indeed inspired by observations of the near wall region of turbulent flows[28] and wavy streaks and streamwise vortices are ubiquitous features in that region.[38] From a more fluid dynamical point of view, as opposed to low-order nonlinear dynamics, the suggestion[26] is that the process can only be self-sustaining in a well-defined range of scales. If the scales are too small, viscous relaxation dominates. If the scales are too large, the process is destroyed by secondary instabilities. Thus the process would be observed only in a small region near the wall. The critical scales for the self-sustaining process would then control the size of the turbulent boundary layer and the streak spacing of 100 wall units. The latter should be considered as a critical Reynolds number for self-sustenance.[26,30] This is nothing but Malkus's *marginal stability* ideas[52] applied to the nonlinear instability process described in this paper.

ACKNOWLEDGMENTS

Fabian Waleffe

APPENDIX: COEFFICIENTS

For the reduction (17) the coefficients in model (20) are

$$\sigma_m = \alpha\beta^2\delta_1/(\kappa_b\kappa_d\delta_3),$$

$$\sigma_u = \beta\gamma/\kappa_v,$$

$$\sigma_v = \alpha^2\beta(\alpha^2\kappa_b + \delta_1\delta_2\kappa_d)/(\gamma\kappa_b\kappa_d\kappa_v\delta_3), \qquad (A1)$$

$$\sigma_w = (\alpha\delta_1/\kappa_b + \alpha\delta_2/\kappa_d)/2,$$

$$\kappa_w^2 = (2\gamma^2\delta_3^2 + \beta^2\kappa_d^2)/(2\delta_3^2),$$

with $\quad \delta_1^2 = \gamma^2 - \alpha^2 > 0, \qquad \delta_2^2 = \gamma^2 - \beta^2 - \alpha^2 > 0 \qquad$ and $\delta_3^2 = \gamma^2 + \beta^2 - \alpha^2$, while for the reduction (19) they are

$$\sigma_m = \alpha\beta\delta_1/(2\kappa_b\kappa_c),$$

$$\sigma_u = \beta\gamma/\kappa_v,$$

$$\sigma_v = \alpha^2(\gamma^2 - \beta^2)/(2\gamma\kappa_c\kappa_v), \qquad (A2)$$

$$\sigma_w = \alpha\delta_1/(2\kappa_b),$$

$$\kappa_w^2 = (\gamma^2 + \kappa_d^2)/2,$$

with $\delta_1^2 = \gamma^2 - \alpha^2 > 0$ and $\gamma^2 - \beta^2 > 0$ otherwise feedback is not possible.

[1] The linear stability analysis has actually led to some remarkable results and is a lot more involved than suggested by that sentence. Rayleigh (1880) showed that velocity profiles without inflection points cannot be unstable in the inviscid limit, $R \to \infty$, but Heisenberg (1925), Tollmien (1927) and Lin (1945) demonstrated that viscous effects could lead to linear instability of noninflectional profiles. Nonetheless, for all its mathematical and physical interest, the linear viscous instability does not explain the observations. The viscous instability does not occur for Couette and pipe flow, while in plane Poiseuille flow, it occurs at a Reynolds number $R_L = 5772$, much larger than the observed $R_c \approx 1000$. The linear viscous instability is more significant for boundary layers. See Ref. 2.

[2] P. G. Drazin and W. V. R. Reid, *Hydrodynamic Stability* (Cambridge University Press, Cambridge, 1981).

[3] J. Serrin, "On the stability of viscous fluid motions," Arch. Rat. Mech. Anal. **3**, 1 (1959).

[4] D. D. Joseph, "Stability of fluid motion," *Springer Tracts in Natural Philosophy* (Springer-Verlag, Berlin, 1976), Vols. 27 and 28.

[5] W. V. R. Malkus and G. Veronis, "Finite amplitude cellular convection," J. Fluid Mech. **4**, 225 (1958).

[6] J. T. Stuart, "On the nonlinear mechanics of wave disturbances in stable and unstable parallel flows. Part 1. The basic behavior in plane Poiseuille flow," J. Fluid Mech. **9**, 353 (1960).

[7] P. Manneville, *Dissipative Structures and Weak Turbulence* (Academic, Boston, 1990).

[8] S. A. Orszag and A. T. Patera, "Secondary instability of wall-bounded shear flows," J. Fluid Mech. **128**, 347 (1983).

[9] T. Herbert, "Secondary instability of plane channel flow to subharmonic three-dimensional disturbances," Phys. Fluids **26**, 871 (1983).

[10] B. J. Bayly, S. A. Orszag, and T. Herbert, "Instability mechanisms in shear flow transition," Annu. Rev. Fluid Mech. **20**, 359 (1988).

[11] F. Waleffe, "On the 3D instability of strained vortices," Phys. Fluids A, **2**, 76 (1990).

[12] P. J. Schmid and D. S. Henningson, "A new mechanism for rapid transition involving a pair of oblique waves," Phys. Fluids A **4**, 1986 (1992).

[13] K. M. Butler and B. F. Farrell, "Three-dimensional optimal perturbations in viscous shear flows," Phys. Fluids A **4**, 1637 (1992).

[14] L. N. Trefethen, A. E. Trefethen, S. C. Reddy, and T. A. Driscoll, "Hydrodynamic stability without eigenvalues," Science **261**, 578 (30 July 1993).

[15] B. F. Farrell and P. J. Ioannou, "Stochastic forcing of the linearized Navier–Stokes equations," Phys. Fluids A **5**, 2600 (1993).

[16] D. J. Benney and L. H. Gustavsson, "A new mechanism for linear and non-linear hydrodynamic instability," Stud. Appl. Math. **64**, 185 (1981).

[17] L. H. Gustavsson, "Energy growth of three-dimensional disturbances in plane Poiseuille flow," J. Fluid Mech. **224**, 241 (1991).

[18] F. Waleffe, "Hydrodynamic stability and turbulence: Beyond transients to a self-sustaining process," Stud. Appl. Math. **95**, 319 (1995).

[19] F. Waleffe, "Transition in shear flows. Nonlinear normality versus non-normal linearity," Phys. Fluids **7**, 3060 (1995).

[20] O. Dauchot and P. Manneville, "Local versus global concepts in hydrodynamic stability theory," J. Phys. II (France) **7**, 371 (1997).

[21] T. Gebhardt and S. Grossmann, "Chaos transition despite linear stability," Phys. Rev. E **50**, 3705 (1994).

[22] J. S. Baggett, T. A. Driscoll, and L. N. Trefethen, "A mostly linear model of transition to turbulence," Phys. Fluids **7**, 833 (1995).

[23] W. V. R. Malkus and D. B. Zaff (see Zaff's thesis, MIT Department of Mathematics, 1987).

[24] M. Nagata, "Three-dimensional finite-amplitude solutions in plane Couette flow: Bifurcation from infinity," J. Fluid Mech. **217**, 519 (1990).

[25] R. M. Clever and F. H. Busse, "Three-dimensional convection in a horizontal layer subjected to constant shear," J. Fluid Mech. **234**, 511 (1992).

[26] F. Waleffe, J. Kim, and J. Hamilton, "On the origin of streaks in turbulent shear flows," in *Turbulent Shear Flows 8: Selected papers from the 8th International Symposium on Turbulent Shear Flows*, Munich, Germany, 9–11 September 1991, edited by F. Durst, R. Friedrich, B. E. Launder, F. W. Schmidt, U. Schumann, and J. H. Whitelaw (Springer-Verlag, Berlin, 1993), pp. 37–49.

[27] J. Hamilton, J. Kim, and F. Waleffe, "Regeneration mechanisms of near-wall turbulence structures," J. Fluid Mech. **287**, 317 (1995).

[28] M. S. Acarlar and C. R. Smith, "A study of hairpin vortices in a laminar boundary layer," J. Fluid Mech. **175**, 1, 43 (1987).

[29] D. J. Benney, "The evolution of disturbances in shear flows at high Reynolds numbers," Stud. Appl. Math. **70**, 1 (1984).

[30] J. Jimenez and P. Moin, "The minimal flow unit in near-wall turbulence," J. Fluid Mech. **225**, 213 (1991).

[31] N. Tillmark and P. H. Alfredsson, "Experiments on transition in plane Couette flow," J. Fluid Mech. **235**, 89 (1992).

[32] F. Daviaud, J. Hegseth, and P. Bergé, "Subcritical transition to turbulence in plane Couette flow," Phys. Rev. Lett. **69**, 2511 (1992).

[33] O. Dauchot and F. Daviaud, "Finite amplitude perturbation and spot growth mechanism in plane Couette flow," Phys. Fluids **7**, 335 (1995).

[34] A. Lundbladh and A. Johansson, "Direct simulation of turbulent spots in plane Couette flow," J. Fluid Mech. **229**, 499 (1991).

[35] A. Conley and H. B. Keller, "Wavy-Taylor vortices in plane Couette flow," preprint MCS-P495-0195, Argonne National Laboratory, 1995.

[36] C. R. Smith and S. P. Metzler, "The characteristics of low-speed streaks in the near-wall region of a turbulent boundary layer," J. Fluid Mech. **129**, 27 (1983).

[37] F. H. Busse, "Bounds for turbulent shear flow," J. Fluid Mech. **41**, 219 (1970).

[38] D. D. Stretch, "Automated pattern eduction from turbulent flow diagnostics," Annual Research Briefs—1990, Center for Turbulence Research, Stanford University.

[39] M. R. Head and P. Bandyopadhyay, "New aspects of turbulent boundary layer structure," J. Fluid Mech. **107**, 297 (1981).

[40] M. Nagata, "Time-dependent 3D solutions in plane Couette flow," preprint (1996).

[41] Nonlinearity in fluid dynamics typically takes the form of *triad* interactions (e.g., Ref. 43): $(d/dt + \kappa_m^2/R)M = \sigma_m XY + (\kappa_m^2/R)M_0$, $(d/dt + \kappa_x^2/R)X = \sigma_x MY$, $(d/dt + \kappa_y^2/R)Y = \sigma_y MX$, where $\sigma_m + \sigma_x + \sigma_y = 0$ for energy conservation. Linearizing around the laminar solution $M = M_0$, $X = Y = 0$ yields $(d/dt + \kappa_y^2/R)(d/dt + \kappa_x^2/R)X = \sigma_x\sigma_y M_0^2 X$ with instability if $\sigma_x\sigma_y > 0$ and stability if $\sigma_x\sigma_y < 0$. Transient growth corresponds to the crossover when one coefficient is equal to zero, $\sigma_y = 0$ say, but then, there is no nonlinear feedback on Y that decays viscously and $\sigma_x = -\sigma_m$ by energy conservation. The only (not-so-)nonlinear effect triggered by the transient growth of X is to reduce the mean M thus stopping the growth (see also Refs. 18 and 19). The laminar state is the global attractor unless $R > R_c = (\kappa_x\kappa_y)/(M_0\sqrt{\sigma_x\sigma_y})$ which is real and finite only in the unstable case $\sigma_x\sigma_y > 0$.

[42] S. Reddy, P. J. Schmid, and J. S. Baggett, "On stability of streamwise streaks and transition to turbulence in plane channel flow," submitted to J. Fluid Mech.

Phys. Fluids, Vol. 9, No. 4, April 1997

Fabian Waleffe   899

[43] F. Waleffe, ''The nature of triad interactions in homogeneous turbulence,'' Phys. Fluids A **4**, 350 (1992).

[44] N. Aubry, P. Holmes, J. L. Lumley, and E. Stone, ''The dynamics of coherent structures in the wall region of a turbulent boundary layer,'' J. Fluid Mech. **192**, 115 (1988).

[45] S. Sanghi and N. Aubry, ''Mode interaction models for near-wall turbulence,'' J. Fluid Mech. **247**, 455 (1993).

[46] X. Zhou and L. Sirovich, ''Coherence and chaos in a model of turbulent boundary layer,'' Phys. Fluids A **4**, 2855 (1992).

[47] L. Sirovich and X. Zhou, ''Dynamical model of wall-bounded turbulence,'' Phys. Rev. Lett. **72**, 340 (1994).

[48] S. H. Strogatz, *Nonlinear Dynamics and Chaos* (Addison-Wesley, Reading, MA, 1994).

[49] O. Dauchot and F. Daviaud, ''Streamwise vortices in plane Couette flow,'' Phys. Fluids **7**, 901 (1995).

[50] O. Dauchot, S. Bottin, and F. Daviaud, ''Streamwise vortices: A finite amplitude solution from forced to pure plane Couette flow,'' submitted to J. Fluid Mech.

[51] F. Waleffe (unpublished).

[52] W. V. R. Malkus, ''Outline of a theory of turbulent shear flow,'' J. Fluid Mech. **1**, 521 (1956).